$^{40}Ar/^{39}Ar$ Geochronology Results from the Veyo, Gunlock, Billies Mountain, The Flat Tops, Maple Ridge, Hebron, Enterprise, and Central West Quadrangles, Utah

by

Utah Geological Survey and
New Mexico Geochronology Research Laboratory

Bibliographic citation for this data report:

Utah Geological Survey and New Mexico Geochronology Research Laboratory, 2007, $^{40}Ar/^{39}Ar$ geochronology results from the Veyo, Gunlock, Billies Mountain, The Flat Tops, Maple Ridge, Hebron, Enterprise, and Central West quadrangles, Utah: Utah Geological Survey Open-File Report 513, variously paginated, also available online, <http://geology.utah.gov/online/ofr/ofr-513.pdf>.

OPEN-FILE REPORT 513
UTAH GEOLOGICAL SURVEY
a division of
Utah Department of Natural Resources
2008

This Open-File Report makes available raw analytical data from laboratory procedures completed to determine the age of rock samples collected during geologic mapping funded or partially supported by the Utah Geological Survey (UGS). The references listed in table 1 report the age of the samples and provide additional information such as the sample location, geologic setting, and significance or interpretation of the samples in the context of the area in which they were collected. This report was prepared by the New Mexico Geochronology Research Laboratory under contract to the UGS. These data are highly technical in nature and proper interpretation requires considerable training in the applicable geochronologic techniques.

Disclaimer

This Open-File release is intended as a data repository for technical analytical information gathered in support of various geologic mapping projects. The data are presented as received from the New Mexico Geochronology Research Laboratory and do not necessarily conform to UGS technical or editorial standards. Therefore, it may be premature for an individual or group to take actions based on the contents of this report.

Although this product represents the work of professional scientists, the Utah Department of Natural Resources, Utah Geological Survey, makes no warranty, expressed or implied, regarding its suitability for a particular use. The Utah Department of Natural Resources, Utah Geological Survey, shall not be liable under any circumstances for any direct, indirect, special, incidental, or consequential damages with respect to claims by users of this product.

References to geologic reports that cite or explain samples analyzed in this report

Biek, R.F., Rowley, P.D., Hacker, D.B., Hayden, J.M., Willis, G.C., Hintze, L.F., Anderson, R.E., and Brown, K.D., 2007, Interim geologic map of the St. George 30' x 60' quadrangle, Washington and Iron Counties, Utah: Utah Geological Survey Open-File Report 478, 70 p., 2 plates., scale 1:100,000.

Constenius, K.N., Coogan, J.C., and Biek, R.F., 2006, Progress report geologic map of the east part of the Provo 30' x 60' quadrangle, Utah and Wasatch Counties, Utah: Utah Geological Survey Open-File Report 490, 31 p., 1 plate, scale 1:62,500.

Doelling, H.H., 2004, Interim geologic map of the east half of the Salina 30'x60' quadrangle, Emery, Sevier, and Wayne Counties, Utah: Utah Geological Survey Open-File Report 438, scale 1:62,500.

Hayden, J.M., in preparation, Geologic map of the Veyo quadrangle, Washington County, Utah: Utah Geological Survey Map, 2 plates, scale 1:24,000.

Higgins, J.M., 2002, Interim geologic map of the Veyo quadrangle, Washington County, Utah: Utah Geological Survey Open-File Report 401, scale 1:24,000. (Note: This map does not include discussion of new $^{40}Ar/^{39}Ar$ ages.)

Rowley, P.D., Williams, V.S., Vice, G.S., Maxwell, D.J., Hacker, D.B., Snee, L.W., and Mackin, J.H., 2006, Interim geologic map of the Cedar City 30' x 60' quadrangle, Iron and Washington Counties, Utah: Utah Geological Survey Open-File Report 476DM, scale 1:100,000.

Table 1. Sample numbers and locations.

Sample #	7.5' quadrangle	Latitude (N)	Longitude (W)	Reference
VY11802-1	Veyo	37.367	113.631	Higgins (2002), Hayden (in prep.)
VY11702-1	Gunlock	37.281	113.761	Higgins (2002), Hayden (in prep.)
VY8301-4	Veyo	37.350	113.672	Higgins (2002), Hayden (in prep.)
VY8301-9	Veyo	37.323	113.668	Higgins (2002), Hayden (in prep.)
VY122001-1	Veyo	37.252	113.630	Higgins (2002), Hayden (in prep.)
VY122001-4	Veyo	37.309	113.648	Higgins (2002), Hayden (in prep.)
VY122001-3	Veyo	37.312	113.640	Higgins (2002), Hayden (in prep.)
VY122001-9	Veyo	37.310	113.686	Higgins (2002), Hayden (in prep.)
VY11802-7	Veyo	37.371	113.672	Higgins (2002), Hayden (in prep.)
KNC101701-1	Billies Mountain	40° 04' 23.3"	111° 27' 21.4"	Constenius and others (2006)
KNC101701-4	Billies Mountain	40° 04' 02.3"	111° 26' 22.7"	Constenius and others (2006)

Latitude and longitude in NAD83.

Sample #	7.5' quadrangle	Location	Reference
SRD-0101	The Flat Tops	center of sec. 25, R13E T26S	Doelling (2004)
01RB-043	Maple Ridge	SE1/4SW1/4 sec. 12, R18W T39S	Biek and others (2007)
01RB-061	Hebron	NW1/4NE1/4 sec. 3, R18W T38S	Rowley and others (2006)
01RB-062	Enterprise	SE1/4NE1/4 sec. 11, R17W T37S	Rowley and others (2006)
01RB-063	Hebron	NW1/4SE1/4 sec. 5, R17W T38S	Rowley and others (2006)
01RB-064	Hebron	NW1/4SE1/4 sec. 5, R17W T38S	Rowley and others (2006)
01RB-065	Enterprise	NE1/4SE1/4 sec. 27, R17W T37S	Rowley and others (2006)
01RB-066	Hebron	NW1/4SE1/4 sec. 17, R17W T37S	Rowley and others (2006)
01RB-067	Central West	SW1/4SW1/4 sec. 15, R17W T39S	Biek and others (2007)
01RB-068	Central West	NW1/4NE1/4 sec. 34, R16W T38S	Biek and others (2007)

$^{40}Ar/^{39}Ar$ Geochronology Results from the Veyo Quadrangle and the Bull Valley Mountains

By

Lisa Peters

OCTOBER 29, 2002

Prepared for

Robert Biek
Utah Geological Survey
1594 West North Temple, Suite 3110
PO Box 146100
Salt Lake City, Utah 84114-6100

NEW MEXICO
GEOCHRONOLOGY RESEARCH LABORATORY
(NMGRL)

Internal Report #: NMGRL-IR-284

Introduction

Eighteen volcanic samples from the Veyo quadrangle and Bull Valley Mountains of southwestern Utah were submitted for analysis by Bob Biek of the Utah Geological Survey. Groundmass concentrates were prepared from nine basalts from the Veyo quadrangle (VY11802-1, VY11702-1, VY8301-4, VY8301-9, VY122001-1, VY122001-1, VY122001-3, VY122001-4 and VY122001-9) and 3 from the Bull Valley Mountains (01RB063, 01RB065 and 01RB068). A mineral separate of sanidine, biotite or hornblende was prepared from each of the remaining samples (01RB043, 01RB066, 01RB062 and VY11802-7). Under a separate cover letter, four additional samples were submitted. Biotite was separated from samples SRD 0101(a dike) and KNC101701-4 (a tuffaceous clast) and sanidine from KNC101701-4 (a tuffaceous sandstone). The fourth sample was assumed to be middle to late Proterozoic and will be analyzed at a later date.

$^{40}Ar/^{39}Ar$ Analytical Methods and Results

Sanidine from samples KNC101701-1, 01RB061, 01RB064, and 01RB067 and biotite from KNC101701-4 were analyzed by the single crystal total fusion method. The rest of the samples were analyzed as bulk separates with the furnace incremental-heating age spectrum method. Abbreviated analytical methods for the dated samples and a summary of the $^{40}Ar/^{39}Ar$ ages can be found in Table 1. The $^{40}Ar/^{39}Ar$ analytical results are given in Tables 2 and 3. Details of the overall operation of the New Mexico Geochronology Research Laboratory are provided in the Appendix.

All analyzed sanidine crystals from KNC101701-1 yield a Gaussian population with an MSWD of 1.8 (Figure 1). The weighted mean age calculated for this sample is 34.86±0.08 Ma.

The analyzed sanidine from samples 01RB061, 01RB064 and 01RB067 yield populations outside the 95% confidence interval (Figures 2, 3 and 4). Weighted mean ages are calculated for samples 01RB061 and 01RB067 from all of the analyzed crystals at 11.84±0.05 Ma and 14.45±0.06 Ma, respectively. The MSWD values are slightly above the acceptable value (01RB061, 3.2 and 01RB067, 2.6) so the errors have been increased accordingly. A statistical outlier with a relatively small Ar signal size has been eliminated from the weighted mean age calculation of sample 01RB064. Even with the elimination of this point, the MSWD value calculated for this sample (9.3) is higher than the values calculated for any of the other sanidines in this study.

All fourteen analyzed biotite crystals from sample KNC101701-4 have been used to calculate a weighted mean age of 37.18±0.38 Ma (Figure 5). It is noted that the Ar signal sizes are 1 to 2 orders of magnitude smaller than those for the sanidine analyses. As a result, the error is an order of magnitude larger due to increased sensitivity to applicable corrections.

Groundmass concentrate separated from sample VY11802-1 yielded a concordant age spectrum (Figure 6a). A weighted mean age of 1.97±0.02 Ma is calculated from 100% of the ^{39}Ar released. Inverse isochron analysis reveals an atmospheric intercept ($^{40}Ar/^{36}Ar$ = 295.5) and an isochron age that agrees within error to the weighted mean age calculated from the age spectrum (Figure 6b).

Five groundmass concentrates from the Veyo quadrangle (VY11702-1, VY8301-4, VY8301-9, VY122001-1, and VY122001-4) and three from the Bull Valley Mountains (01RB063, 01RB065 and 01RB068) yield age spectra that are well-behaved over the first 80-95% of the ^{39}Ar released during step-heating (Figures 7a-14a). Weighted mean ages are assigned to these well-behaved portions of these age spectra. The remaining steps reveal a dramatic increase in apparent age correlated with a decrease in radiogenic yield and K/Ca ratio. Inverse isochron analysis reveals atmospheric intercepts and isochron ages that agree with the ages calculated from the age spectra (Figures 7b-14b). An exception is the inverse isochron for 01RB063 (Figure 12), the uniformly low radiogenic yields result in a clustering of points and although the $^{40}Ar/^{36}Ar$ intercept is above the atmospheric intercept, very little confidence is put in this value.

Biotite from samples 01RB066 and 01RB043 yield similar age spectra (Figures 15a and 16a) with the first 5-10% revealing increasing radiogenic yields and K/Ca ratios and, in general, increasing apparent ages with the remainder of the age spectra being nearly flat. A weighted mean age of 21.65±0.09 Ma is calculated from the last ~96% of the ^{39}Ar released during the heating of 01RB043, and an acceptable MSWD value of 1.8 is calculated for this age. The final ~90% of ^{39}Ar released from 01RB066 biotite is used to calculate a weighted mean age of 20.71±0.10 Ma. The MSWD value for this age is slightly outside the 95% confidence interval (2.9). Inverse isochron analysis of 01RB066 (Figure 15b) reveals an atmospheric intercept (293±23) and an isochron age that agrees within error to the age calculated from the age spectrum. The $^{40}Ar/^{36}Ar$ intercept (Figure 16b) for sample 01RB043 (286±14) is slightly below the atmospheric intercept value but the isochron age is within error of the weighted mean age calculated from the age spectrum.

Biotite and hornblende from 01RB062 were analyzed. The biotite yielded increasing radiogenic yields, K/Ca ratios and apparent ages over the first ~33% of ^{39}Ar

released (Figure 17a). The remaining 67% of the ^{39}Ar yields concordant ages and an apparent age of 20.51±0.04 Ma is calculated for this portion of the age spectrum. It is noted that the radiogenic yields continue to rise throughout this later portion of the age spectrum. Inverse isochron analysis reveals a ^{40}Ar/^{36}Ar intercept within error of atmosphere and an isochron age within error of the age calculated from the age spectrum (Figure 17b). The 01RB062 hornblende age spectrum is somewhat disturbed and reveals increasing radiogenic yields and decreasing K/Ca ratios over the first ~35% (Figure 18a). Steps H and I contain the next 60% of ^{39}Ar released and were used to calculate a weighted mean age of 21.07±0.15 Ma. The remaining steps yield a slight increase in apparent age and a decrease in radiogenic yield and K/Ca ratio. Inverse isochron analysis reveals an atmospheric intercept that is suggestive of excess Ar (^{40}Ar/^{36}Ar = 306±13) and an isochron age that agrees within error to the weighted mean age calculated from the age spectrum (21.12±0.35 Ma), but with an error three times the magnitude (Figure 18b).

Biotite from SRD-0101 yielded an age spectrum similar to the 01RB062 biotite age spectrum with increasing radiogenic yields and K/Ca ratios over the first ~25% of the ^{39}Ar released during heating (Figure 19a). A weighted mean age of 20.93±0.33 Ma is calculated from the next ~83% of ^{39}Ar released although the MSWD value is outside the 95% confidence interval (8.9). The last four steps of the age spectrum (steps I-L) reveal an increase in apparent age and radiogenic yield and a decrease in K/Ca ratio. Inverse isochron analysis reveals an atmospheric intercept and an isochron age that agrees within error to the weighted mean age calculated from the age spectrum (Figure 19b).

The final three samples (VY122001-3, VY122001-9 and VY11802-7) yield disturbed age spectra (Figure 20-22). VY11802-7 hornblende yielded an age spectrum with rapidly increasing radiogenic yields, decreasing K/Ca ratios and oscillating apparent ages over the first ~25% of ^{39}Ar released during heating (Figure 20a). A weighted mean age of 1.77±0.09 Ma is calculated from the next ~71% of ^{39}Ar released. The remaining 5% of the age spectrum reveals a drop in apparent age, radiogenic yield and K/Ca ratio. Inverse isochron analysis reveals an atmospheric intercept and an isochron age that agrees within error to the age calculated from the age spectrum (Figure 20b). Groundmass concentrate from VY122001-3 yields apparent ages that decrease over the first ~50% of the spectrum followed by an increase in apparent ages over the remainder of the age spectrum (Figure 21a). Radiogenic yields are low (<11%) throughout the age spectrum and K/Ca ratios decrease steadily. A weighted mean age of 0.74±0.07 Ma is calculated for steps C-G, this age has an acceptable MSWD value of 1.2. Inverse isochron analysis of steps C-I reveals a ^{40}Ar/^{36}Ar intercept greater than the atmospheric intercept (303.6±2.8) and an isochron age of 0.47±0.12 Ma (Figure 21b). VY122001-9 groundmass yields increasing apparent ages and decreasing K/Ca ratios throughout the entire heating schedule (Figure 22a). The radiogenic yields increase over the first 75% of the ^{39}Ar released and then decrease over the remaining portion of the age spectrum. Inverse isochron analysis reveals an atmospheric intercept (Figure 22b).

Discussion

Most of the samples from the Veyo quadrangle and Bull Valley Mountains provided low complexity results that can be interpreted in a straightforward manner. The ages assigned to all Bull Valley Mountains and Veyo Quadrangle samples are summarized in Figures 23 and 24. The ages assigned to samples 01RB061, 01RB064 and 01RB067 (the rhyolitic samples analyzed with sanidine) provide eruption ages for the units from which they were sampled. The spread in ages revealed by the analyzed crystals of 01RB064 is larger than the spread in ages seen for the analyzed crystals of either 01RB061 or 01RB067. It is noted that the analyses of 01RB064 display a correlation between an increase in apparent age and larger radiogenic yields. This suggests that there has been slight alteration and accompanying Ar loss (Deino and Potts, 1990). Groundmass from samples VY11802-1, VY11702-1, VY8301-4, VY8301-9, VY122001-1, VY122001-4, 01RB063, 01RB065, and 01RB068 are also thought to provide accurate eruption ages for these units. The rise in apparent age correlated with a decrease in both radiogenic yield and K/Ca ratio revealed in the last 5-15% of all of these samples, except VY11802-1, is thought to be due to excess Ar in high Ca, high temperature degassing phenocrysts (such as olivine and pyroxene). The atmospheric $^{40}Ar/^{36}Ar$ intercepts of the inverse isochrons suggests that the lower temperature steps do not contain excess Ar, thus we feel confident in assigning the weighted mean ages calculated from the age spectra as the eruption ages of these samples. The increasing apparent ages, radiogenic yields and K/Ca ratios revealed in the early heating steps of the biotite age spectra from samples 01RB043, 01RB066 and 01RB062 suggest alteration of the mineral separates. The alteration appears minimal for samples 01RB043 and 01RB066 with ≤ 10% of the spectrum affected and we feel fairly confident in assigning the weighted mean ages as the eruption ages of these units. Alteration of 01RB062 appears more significant with ~30% of the spectrum affected. Because the age spectrum from 01RB062 hornblende is also somewhat disturbed we suggest that geological information may be useful in deciding which apparent age provides the more accurate eruption age for the andesite from which 01RB062 was sampled. The remaining three Veyo quadrangle samples (VY11802-7, and VY122001-3, VY122001-9) provide lower quality analyses. The very low radiogenic yields (≤ ~25 %) correlated with decreasing K/Ca ratios and oscillating apparent ages suggests that the disturbed nature of VY11802-7 age spectrum is due to either alteration of the sample or to material such as glass adhering to the hornblende. Our preferred hypothesis to explain the disturbed nature of the VY122001-3 age spectrum is that it contains excess Ar like many of the other Veyo quadrangle samples, with the first two steps affected as well the later steps. The isochron age (0.47±0.12 Ma) is assigned as our best estimate of the eruption age of VY122001-3. Alternatively, the disturbed age spectrum could be the result of ^{39}Ar recoil superimposed on an age spectrum affected by excess Ar, similar to others in this study. During irradiation, the ^{39}Ar produced may recoil out of the high K phases and into the lower K phases, thus increasing the apparent age of the high K phases and lowering the apparent age of the lower K phases (Figure 25). The preferred explanation for the disturbed VY122001-9 age spectrum is a combination of Ar loss associated with alteration and excess Ar. The increasing radiogenic yields and apparent ages revealed in the first ~70% of ^{39}Ar released suggests alteration while the decreasing radiogenic yields and K/Ca ratios and increasing apparent ages is suggestive of excess Ar.

Samples KNC101701-1 and KNC101701-4 (34.86±0.08 Ma and 37.18±0.38 Ma, respectively) provide maximum ages for the Tibble Fork Formation. Although these ages do not agree within error, they are consistent with the KNC101701-4 biotite (the older apparent age) coming from a tuffaceous clast at the base of the Tibble Fork Formation and the KNC101701-1 sanidine coming from a stratigraphically higher tuffaceous sandstone within the Tibble Fork Formation. The weighted mean age of 34.50±0.28 Ma provides an apparent age that corresponds to the time when the biotite in the dike cooled below the biotite closure temperature of 300-350 C. This suggests the dike is related to the Henry Mountain intrusions rather than the dike swarms in the southern San Rafael Swell/Capitol Reef Mountain National Park area.

References Cited

Deino, A., and Potts, R., 1990. Single-Crystal $^{40}Ar/^{39}Ar$ dating of the Olorgesailie Formation, Southern Kenya Rift, J. Geophys. Res., 95, 8453-8470.

Mahon, K.I., 1996. The New "York" regression: Application of an improved statistical method to geochemistry, International Geology Review, 38, 293-303.

Samson, S.D., and, Alexander, E.C., Jr., 1987. Calibration of the interlaboratory $^{40}Ar/^{39}Ar$ dating standard, Mmhb-1, Chem. Geol., 66, 27-34.

Steiger, R.H., and Jäger, E., 1977. Subcommission on geochronology: Convention on the use of decay constants in geo- and cosmochronology. Earth and Planet. Sci. Lett., 36, 359-362.

Taylor, J.R., 1982. An Introduction to Error Analysis: The Study of Uncertainties in Physical Measurements,. Univ. Sci. Books, Mill Valley, Calif., 270 p.

York, D., 1969. Least squares fitting of a straight line with correlated errors, Earth and Planet. Sci. Lett., 5, 320-324.

Table 1. Summary of $^{40}Ar/^{39}Ar$ data and analytical methods.

Sample	Unit/Location	Irradiation	mineral	analysis	# of steps/crystals	MSWD	Age	±2σ	Comments
KNC101701-1	Tibble Fork Formation	NM-152	sanidine	laser total fusion	15	1.8	34.86	0.08	
KNC101701-4	Tibble Fork Formation	NM-152	biotite	laser total fusion	14	1.7	37.18	0.38	
01RB061	Bull Valley Mountains	NM-152	sanidine	laser total fusion	15	3.2**	11.84	0.05	
01RB064	Bull Valley Mountains	NM-152	sanidine	laser total fusion	15	9.3**	6.05	0.05	
01RB067	Bull Valley Mountains	NM-152	sanidine	laser total fusion	15	2.6**	14.45	0.06	
01RB063	Bull Valley Mountains	NM-153	groundmass concentrate	furnace step-heat	6	2.2	0.42	0.13	
01RB065	Bull Valley Mountains	NM-153	groundmass concentrate	furnace step-heat	7	4.6**	1.08	0.04	
01RB068	Bull Valley Mountains	NM-153	groundmass concentrate	furnace step-heat	7	2.6**	2.22	0.05	
01RB043	Bull Valley Mountains	NM-152	biotite	furnace step-heat	8	1.8	21.65	0.09	
01RB066	Bull Valley Mountains	NM-152	biotite	furnace step-heat	6	2.9**	20.71	0.10	
01RB062	Bull Valley Mountains	NM-152	hornblende	furnace step-heat	2	0.25	21.07	0.15	
01RB062	Bull Valley Mountains	NM-152	biotite	furnace step-heat	6	1.20	20.51	0.08	
VY11802-1	Veyo quadrangle	NM-153	groundmass concentrate	furnace step-heat	9	1.9	1.97	0.02	
VY11702-1	Veyo quadrangle	NM-153	groundmass concentrate	furnace step-heat	7	3.8**	0.98	0.03	
VY8301-4	Veyo quadrangle	NM-153	groundmass concentrate	furnace step-heat	7	3.9**	1.98	0.04	
VY8301-9	Veyo quadrangle	NM-153	groundmass concentrate	furnace step-heat	6	6.0**	1.62	0.02	
VY122001-1	Veyo quadrangle	NM-153	groundmass concentrate	furnace step-heat	6	2.1	0.05	0.07	
VY122001-4	Veyo quadrangle	NM-153	groundmass concentrate	furnace step-heat	5	0.25	0.59	0.02	
VY122001-3	Veyo quadrangle	NM-153	groundmass concentrate	furnace step-heat	5	1.2	0.47	0.12	isochron
VY122001-9	Veyo quadrangle	NM-153	groundmass concentrate	furnace step-heat	-	-	-	-	disturbed age spectrum
VY11802-7	Veyo quadrangle	NM-152	hornblende	furnace step-heat	2	0.67	1.77	0.09	
SRD-0101	San Rafael Desert	NM-152	groundmass concentrate	furnace step-heat	5	8.9**	20.93	0.33	

** MSWD outside 95% confidence interval

Notes:

Sample preparation and irradiation:

Mineral separates were prepared using standard crushing, dilute acid treatment and hand-picking techniques.
Mineral separates were loaded into a machined Al disc and irradiated for 14 hours in NM-152 or 1 hour for NM-153 in the D-3 position, Nuclear Science Center, College Station, TX.
Neutron flux monitor Fish Canyon Tuff sanidine (FC-1). Assigned age = 27.84 Ma (Deino and Potts, 1990)
relative to Mmhb-1 at 520.4 Ma (Samson and Alexander, 1987).

Instrumentation:

Mass Analyzer Products 215-50 mass spectrometer on line with automated all-metal extraction system.
Groundmass concentrate, hornblende and biotite separates were step-heated using a Mo double-vacuum resistance furnace. Heating duration in the furnace was 9 or 10 minutes.
Reactive gases removed during furnace analysis by reaction with 3 SAES GP-50 getters, 2 operated at ~450°C and
1 at 20°C. Gas also exposed to a W filiment operated at ~2000°C.
Single crystal sanidine and biotite were fused by a 50 watt Synrad CO_2 laser.
Reactive gases removed during a reaction with 2 SAES GP-50 getters, 1 operated at ~450°C and
1 at 20°C (2 minutes for sanidine, 5 minutes for biotite). Gas also exposed to a W filament operated at ~2000°C and a cold finger operated at -140°C.

Analytical parameters:

Electron multiplier sensitivities: 1.14 x 10^{-16} moles/pA for laser analyses 01RB061, 01RB064, 01RB067 and 1.22 x 10-16 moles/pA for laser analyses KNC101701-1 and KNC101701-4.
Electron multiplier sensitivities: 2.24 x 10^{-16} moles/pA for furnace analyses in NM-152 2.09 x 10-16 moles/pA for furnace analyses in NM-153.
Total system blank and background for furnace analyses averaged 632, 1.1 , 0.3 , 2.0, 2.6 x 10^{-18} moles at masses 40, 39, 38, 37, and 36, respectively
and 98, 2.1, 0.1, 1.3, 0.5 x 10^{-18} moles at masses 40, 39, 38, 37, and 36, respectively for laser analyses.
J-factors determined to a precision of ± 0.1% by CO_2 laser-fusion of 4 single crystals from each of 6 or 4 radial positions around the irradiation tray.
Correction factors for interfering nuclear reactions were determined using K-glass and CaF_2 and are as follows:
$(^{40}Ar/^{39}Ar)_K$ = 0.0002±0.0003; $(^{36}Ar/^{37}Ar)_{Ca}$ = 0.00028±0.000005; and $(^{39}Ar/^{37}Ar)_{Ca}$ = 0.0007±0.00002.

Age calculations:

Total gas age and error calculated by weighting individual steps by the fraction of ^{39}Ar released.
MSWD values are evaluated for n-1 degrees of freedom for weighted mean age.
$^{40}Ar/^{36}Ar_i$ and MSWD values calculated from regression results obtained by the methods of York (1969).
If the MSWD is outside the 95% confidence window (cf. Mahon, 1996; Table 1), the error is multiplied by the square root of the MSWD.
Decay constants and isotopic abundances after Steiger and Jäger (1977).
All final errors reported at ±2σ, unless otherwise noted.

Table 2. Argon isotopic results for single crystal laser analyses.

ID	$^{40}Ar/^{39}Ar$	$^{37}Ar/^{39}Ar$	$^{36}Ar/^{39}Ar$ (x 10^{-3})	$^{39}Ar_K$ (x 10^{-15} mol)	K/Ca	$\%^{40}Ar^*$	Age (Ma)	±1s (Ma)
KNC101701-1, single crystal sanidine, J=0.0014552, D=1.00698, NM-152, Lab#=53153								
03	13.40	0.0069	0.2311	35.6	74.0	99.5	34.65	0.08
01	13.38	0.0051	0.1136	35.4	100.4	99.8	34.72	0.08
08	13.40	0.0049	0.1213	32.1	103.7	99.7	34.76	0.09
13	13.49	0.0049	0.3288	29.0	103.6	99.3	34.81	0.08
09	13.40	0.0055	0.0419	30.3	93.3	99.9	34.82	0.09
11	13.40	0.0050	-0.0044	20.3	102.9	100.0	34.84	0.08
06	13.45	0.0072	0.1692	30.8	71.1	99.6	34.85	0.09
04	13.50	0.0052	0.3131	23.8	97.4	99.3	34.87	0.08
14	13.44	0.0055	0.0792	25.1	92.7	99.8	34.88	0.08
05	13.44	0.0052	0.0599	25.6	98.4	99.9	34.89	0.09
02	13.49	0.0052	0.1998	15.7	98.2	99.6	34.91	0.09
10	13.50	0.0083	0.2226	14.8	61.6	99.5	34.93	0.08
15	13.44	0.0057	-0.0150	20.7	90.2	100.0	34.95	0.08
12	13.50	0.0055	0.0821	12.2	93.5	99.8	35.04	0.08
07	13.51	0.0053	0.0770	7.91	96.8	99.8	35.05	0.09
weighted mean	MSWD = 1.8	n=15			91.9	±12.8	34.86	0.08*
01RB061, single crystal sanidine, J=0.001468, D=1.00712, NM-152, Lab#=53172								
06	4.599	0.0222	0.5600	8.25	23.0	96.4	11.71	0.04
02	4.513	0.0228	0.2134	14.1	22.4	98.6	11.75	0.03
01	4.629	0.0237	0.5630	10.4	21.5	96.4	11.79	0.04
10	4.516	0.0200	0.1659	8.60	25.5	99.0	11.80	0.04
12	4.521	0.0163	0.1583	7.10	31.3	99.0	11.81	0.04
04	4.532	0.0203	0.1898	7.55	25.1	98.8	11.82	0.04
08	4.523	0.0256	0.1422	12.2	19.9	99.1	11.83	0.03
03	4.602	0.0308	0.3645	5.18	16.6	97.7	11.87	0.05
15	4.525	0.0215	0.0983	8.34	23.8	99.4	11.87	0.04
11	4.506	0.0168	0.0276	5.41	30.4	99.8	11.88	0.05
09	4.570	0.0149	0.2301	8.46	34.3	98.5	11.89	0.03
14	4.521	0.0194	0.0638	8.52	26.3	99.6	11.89	0.04
13	4.555	0.0195	0.1736	7.09	26.1	98.9	11.89	0.04
05	4.508	0.0258	-0.0346	5.92	19.7	100.3	11.93	0.04
07	4.581	0.0195	0.1940	5.76	26.2	98.8	11.94	0.04
weighted mean	MSWD = 3.2**	n=15			24.8	±4.7	11.84	0.05*
01RB064, single crystal sanidine, J=0.0014692, D=1.00712, NM-152, Lab#=53174								
16	2.329	0.0076	0.3981	2.70	67.1	95.0	5.85	0.08
10	2.342	0.0061	0.3538	9.59	83.6	95.6	5.92	0.02
04	2.398	0.0093	0.4932	6.66	54.6	94.0	5.96	0.03
09	2.333	0.0062	0.2539	11.2	81.9	96.8	5.98	0.02
11	2.361	0.0083	0.3089	10.3	61.4	96.2	6.01	0.03
05	2.317	0.0073	0.1488	15.2	69.8	98.1	6.02	0.02
06	2.322	0.0056	0.1409	7.58	90.8	98.2	6.04	0.03
14	2.316	0.0052	0.0915	12.8	98.1	98.9	6.06	0.02
07	2.324	0.0085	0.1131	11.4	60.1	98.6	6.06	0.02
02	2.394	0.0114	0.3390	5.46	44.6	95.9	6.07	0.04
08	2.401	0.0099	0.3559	10.1	51.8	95.7	6.08	0.03
03	2.327	0.0095	0.0682	10.3	53.5	99.2	6.11	0.03
12	2.316	0.0131	-0.0096	5.21	38.8	100.2	6.14	0.04
15	2.342	0.0069	0.0536	18.2	74.4	99.3	6.16	0.02
01	2.404	0.0101	0.2492	10.0	50.4	97.0	6.17	0.03
13	*2.448*	*0.0076*	*0.1466*	*5.89*	*67.1*	*98.3*	*6.36*	*0.04*
weighted mean	MSWD =9.3**	n=15			65.4	±17.5	6.05	0.05*

Table 2. Argon isotopic results for single crystal laser analyses.

ID	$^{40}Ar/^{39}Ar$	$^{37}Ar/^{39}Ar$	$^{36}Ar/^{39}Ar$ (x 10^{-3})	$^{39}Ar_K$ (x 10^{-15} mol)	K/Ca	$\%^{40}Ar^*$	Age (Ma)	±1s (Ma)
01RB067, single crystal sanidine, J=0.0014613, D=1.00712, NM-152, Lab#=53167								
02	5.524	0.0029	0.2124	9.34	174.6	98.9	14.34	0.04
10	5.564	0.0039	0.2804	10.0	129.9	98.5	14.39	0.04
14	5.587	0.0030	0.3428	15.1	168.1	98.2	14.40	0.03
04	5.597	0.0039	0.3638	15.9	130.4	98.1	14.42	0.03
12	5.562	0.0040	0.2313	15.3	128.1	98.8	14.43	0.03
11	5.773	0.0045	0.9336	7.36	112.3	95.2	14.44	0.05
15	5.666	0.0039	0.5712	12.7	130.3	97.0	14.44	0.04
08	5.603	0.0032	0.3497	15.4	162.0	98.2	14.44	0.03
06	5.556	0.0031	0.1760	14.2	164.7	99.1	14.45	0.03
05	5.654	0.0033	0.4998	8.41	152.7	97.4	14.46	0.04
03	5.622	0.0034	0.3844	8.14	150.4	98.0	14.46	0.04
07	5.607	0.0061	0.3263	7.92	83.2	98.3	14.47	0.05
13	5.626	0.0034	0.3761	8.52	151.7	98.0	14.48	0.04
01-0	5.596	0.0031	0.1764	13.4	166.7	99.1	14.56	0.03
09	5.743	0.0030	0.6081	8.62	171.1	96.9	14.61	0.05
weighted mean		MSWD =2.6**	n=15		145.1 ±25.6		14.45	0.06*
KNC101701-4, single crystal biotite, J=0.0014541, D=1.00698, NM-152, Lab#=53152								
20	*15.45*	*3.671*	*13.47*	*0.080*	*0.14*	*76.2*	*30.70*	*2.96*
15	16.90	-0.0037	13.70	0.173	-	76.0	33.41	1.30
16	17.05	0.0001	13.15	0.266	4273.1	77.2	34.20	1.08
05	15.16	-0.0028	3.594	0.333	-	93.0	36.60	0.69
18	20.16	0.0219	20.46	0.255	23.3	70.0	36.66	1.41
08	14.63	0.0320	1.687	0.276	15.9	96.6	36.71	0.82
17	15.85	0.0361	5.625	0.254	14.1	89.5	36.84	1.05
19	15.08	0.0217	2.996	0.364	23.6	94.1	36.86	0.74
14	14.97	0.0160	2.185	0.729	31.9	95.7	37.20	0.40
10	22.56	0.0078	27.72	0.327	65.0	63.7	37.30	0.93
21	14.88	0.0122	1.466	0.388	41.7	97.1	37.50	0.68
12	15.58	0.0034	3.761	0.313	149.1	92.9	37.55	0.75
01	14.87	-0.0100	1.210	0.287	-	97.6	37.66	0.73
06	17.73	-0.0098	10.78	0.274	-	82.0	37.76	0.95
03	15.30	-0.0066	2.238	0.550	-	95.7	38.00	0.42
weighted mean		MSWD = 1.7	n=14		515.3 ±1130.3		37.18	0.38*

Notes:
Isotopic ratios corrected for blank, radioactive decay, and mass discrimination, not corrected for interferring reactions.
Individual analyses show analytical error only; plateau and total gas age errors include error in J and irradiation parameters.
n= number of heating steps
D= mass spectrometer discrmination
K/Ca = molar ratio calculated from reactor produced $^{39}Ar_K$ and $^{37}Ar_{Ca}$.
* 2σ error
** MSWD outside 95% confidence interval

Table 3. Argon isotopic results for furnace incremental heating analyses.

ID	Temp (°C)	$^{40}Ar/^{39}Ar$	$^{37}Ar/^{39}Ar$	$^{36}Ar/^{39}Ar$ (x 10^{-3})	$^{39}Ar_K$ (x 10^{-16} mol)	K/Ca	$^{40}Ar^*$ (%)	^{39}Ar (%)	Age (Ma)	±1σ (Ma)
VY11802-1, 193.53 mg groundmass concentrate, J=0.0001119, D=1.00712, NM-153, Lab#=53259-01										
A	650	1548.4	2.294	5180.1	19.1	0.22	1.2	3.8	3.6	1.7
B	730	16.22	1.411	22.44	161.9	0.36	59.8	36.3	1.96	0.02
C	780	13.78	0.9272	14.04	73.7	0.55	70.4	51.1	1.96	0.02
D	830	14.46	0.9785	15.79	73.1	0.52	68.3	65.7	1.99	0.02
E	905	16.18	1.332	21.11	45.3	0.38	62.1	74.8	2.03	0.03
F	1005	22.65	1.839	44.86	42.2	0.28	42.2	83.2	1.93	0.04
G	1105	33.60	2.506	82.33	29.3	0.20	28.2	89.1	1.92	0.06
H	1280	91.90	24.28	282.7	33.7	0.021	11.3	95.9	2.13	0.11
I	1700	115.9	28.90	373.1	20.5	0.018	7.0	100.0	1.67	0.17
total gas age			n=9		498.8	0.36			2.03	0.20*
plateau	MSWD = 1.9		n=9	steps A-I	498.8	0.36		100.0	1.97	0.02*
VY11702-1, 189.35 mg groundmass concentrate, J=0.000112, D=1.00712, NM-153, Lab#=53262-01										
B	700	289.9	2.274	968.2	8.42	0.22	1.4	1.4	0.82	0.43
C	750	44.42	2.074	139.3	2.23	0.25	7.7	1.7	0.69	0.30
D	800	14.35	1.677	31.98	68.0	0.30	35.1	12.9	1.02	0.03
E	875	9.280	1.267	14.93	117.3	0.40	53.6	32.1	1.01	0.02
F	975	8.594	1.120	12.95	183.3	0.46	56.6	62.2	0.98	0.01
G	1075	15.59	0.9795	38.21	104.9	0.52	28.1	79.4	0.89	0.02
H	1250	35.11	2.739	104.2	77.2	0.19	13.0	92.0	0.92	0.04
I	*1670*	*61.57*	*7.649*	*170.3*	*48.6*	*0.067*	*19.3*	*100.0*	*2.41*	*0.08*
total gas age			n=8		610.0	0.37			1.08	0.06*
plateau	MSWD = 3.8**		n=7	steps B-H	561.4	0.40		92.0	0.98	0.03*
VY8301-4, 188.35 mg groundmass concentrate, J=0.0001119, D=1.00712, NM-153, Lab#=53263-01										
B	700	196.3	2.364	625.7	13.3	0.22	5.9	2.0	2.35	0.25
C	750	57.55	2.486	181.7	1.63	0.21	7.0	2.3	0.82	0.34
D	800	27.76	1.866	61.30	60.8	0.27	35.3	11.5	1.98	0.03
E	875	17.75	1.429	26.72	93.2	0.36	56.2	25.7	2.01	0.02
F	975	15.01	1.138	17.83	204.7	0.45	65.5	56.9	1.99	0.01
G	1075	19.61	1.014	34.07	164.3	0.50	49.1	81.9	1.94	0.02
H	1250	61.50	2.230	177.7	80.0	0.23	14.9	94.1	1.85	0.07
I	*1670*	*190.8*	*22.29*	*602.6*	*38.9*	*0.023*	*7.7*	*100.0*	*3.00*	*0.22*
total gas age			n=8		656.9	0.38			2.03	0.08*
plateau	MSWD = 3.9**		n=7	steps B-H	618.0	0.40		94.1	1.98	0.04*
VY8301-9, 193.46 mg groundmass concentrate, J=0.0001118, D=1.00712, NM-153, Lab#=53264-01										
B	700	118.5	1.224	373.7	19.6	0.42	6.9	1.9	1.65	0.17
D	800	15.35	0.7346	24.16	117.3	0.69	53.9	13.2	1.67	0.02
E	875	11.34	0.4721	10.92	246.2	1.1	71.9	36.9	1.64	0.01
F	975	10.12	0.4469	7.272	388.6	1.1	79.1	74.4	1.61	0.01
G	1075	13.87	0.4913	20.31	169.3	1.0	57.0	90.7	1.60	0.02
H	1250	40.39	3.288	113.3	67.0	0.16	17.8	97.2	1.45	0.05
I	*1670*	*214.1*	*19.60*	*657.6*	*29.0*	*0.026*	*10.0*	*100.0*	*4.38*	*0.25*
total gas age			n=7		1036.9	0.95			1.69	0.04*
plateau	MSWD = 6.0**		n=6	steps B-H	1007.9	0.98		97.2	1.62	0.02*

Table 3. Argon isotopic results for furnace incremental heating analyses.

ID	Temp (°C)	$^{40}Ar/^{39}Ar$	$^{37}Ar/^{39}Ar$	$^{36}Ar/^{39}Ar$ (x 10^{-3})	$^{39}Ar_K$ (x 10^{-16} mol)	K/Ca	$^{40}Ar^*$ (%)	^{39}Ar (%)	Age (Ma)	±1σ (Ma)
VY122001-1, 213.31 mg groundmass concentrate, J=0.0001077, D=1.00712, NM-153, Lab#=53230-01										
A	650	699.1	1.543	2352.4	28.5	0.33	0.6	15.7	0.80	0.78
B	730	47.61	3.085	160.0	75.8	0.17	1.2	57.4	0.11	0.06
C	780	40.11	5.461	140.0	12.4	0.093	-2.0	64.3	-0.16	0.10
D	830	34.31	7.994	115.7	23.6	0.064	2.3	77.3	0.15	0.07
E	905	39.43	10.58	137.0	18.9	0.048	-0.4	87.7	-0.03	0.08
F	1005	56.28	12.34	195.8	10.6	0.041	-1.0	93.5	-0.11	0.15
G	*1105*	*80.20*	*10.67*	*263.6*	*5.06*	*0.048*	*4.0*	*96.3*	*0.62*	*0.21*
H	*1280*	*167.8*	*114.5*	*586.8*	*4.30*	*0.004*	*2.3*	*98.7*	*0.81*	*0.32*
I	*1700*	*226.2*	*108.8*	*753.1*	*2.44*	*0.005*	*5.6*	*100.0*	*2.66*	*0.55*
total gas age			n=9		181.6	0.14			0.24	0.40*
plateau		MSWD = 2.1	n=6	steps A-F	169.8	0.15		93.5	0.05	0.07*
VY122001-4, 195.26 mg groundmass concentrate, J=0.0001081, D=1.00712, NM-153, Lab#=53232-01										
B	730	58.25	1.466	187.1	96.8	0.35	5.3	16.1	0.60	0.07
C	780	13.16	0.9013	33.66	9.39	0.57	25.0	17.6	0.64	0.08
D	830	9.350	0.6568	21.54	172.4	0.78	32.5	46.2	0.59	0.01
E	905	8.154	0.8268	17.45	133.3	0.62	37.6	68.3	0.60	0.01
F	1005	17.37	1.344	49.22	85.5	0.38	16.9	82.5	0.57	0.03
G	*1105*	*44.77*	*1.454*	*146.5*	*41.8*	*0.35*	*3.6*	*89.4*	*0.31*	*0.09*
H	*1280*	*88.50*	*7.223*	*289.2*	*23.8*	*0.071*	*4.1*	*93.4*	*0.71*	*0.12*
I	*1700*	*109.3*	*18.54*	*359.1*	*40.0*	*0.028*	*4.3*	*100.0*	*0.93*	*0.14*
total gas age			n=8		603.0	0.51			0.60	0.08*
plateau		MSWD = 0.25	n=5	steps B-F	497.4	0.58		82.5	0.59	0.02*
01RB063,188.52 mg glassy groundmass concentrate, J=0.0001093, D=1.00712, NM-153, Lab#=53235-01										
A	650	812.9	0.5239	2742.3	54.0	0.97	0.3	5.5	0.52	0.89
B	730	99.69	0.2922	331.8	449.6	1.7	1.7	51.3	0.33	0.11
C	780	107.1	0.4164	358.6	88.7	1.2	1.1	60.3	0.23	0.12
D	830	121.5	0.8499	402.2	193.9	0.60	2.2	80.1	0.53	0.13
E	905	195.1	1.397	647.6	99.6	0.37	2.0	90.2	0.76	0.21
F	1005	347.4	1.502	1154.9	44.8	0.34	1.8	94.8	1.24	0.39
G	*1105*	*399.5*	*1.292*	*1313.0*	*22.9*	*0.39*	*2.9*	*97.1*	*2.29*	*0.47*
H	*1280*	*625.1*	*4.252*	*2047.4*	*20.0*	*0.12*	*3.3*	*99.2*	*4.04*	*0.71*
I	*1700*	*467.4*	*10.29*	*1480.3*	*8.14*	*0.050*	*6.6*	*100.0*	*6.11*	*0.58*
total gas age			n=9		981.7	1.1			0.63	0.42*
plateau		MSWD = 2.2	n=6	steps A-F	930.7	1.2		94.8	0.42	0.13*
01RB065, 197.63 mg groundmass concentrate, J=0.0001092, D=1.00712, NM-153, Lab#=53237-01										
A	650	3919.6	2.580	13100.1	28.2	0.20	1.2	3.6	9.6	4.4
B	730	64.75	1.785	200.6	126.6	0.29	8.7	19.8	1.11	0.07
C	780	28.63	1.257	76.73	92.3	0.41	21.2	31.5	1.19	0.03
D	830	16.64	0.8481	37.44	129.5	0.60	33.9	48.1	1.11	0.02
E	905	12.42	0.8885	23.70	149.4	0.57	44.2	67.1	1.08	0.02
F	1005	15.83	1.072	36.33	99.7	0.48	32.7	79.8	1.02	0.02
G	1105	34.52	1.106	98.16	50.0	0.46	16.2	86.2	1.11	0.05
H	*1280*	*91.83*	*6.991*	*278.1*	*44.3*	*0.073*	*11.1*	*91.9*	*2.02*	*0.11*
I	*1700*	*69.09*	*6.213*	*212.8*	*63.7*	*0.082*	*9.7*	*100.0*	*1.33*	*0.08*
total gas age			n=9		783.7	0.41			1.48	0.40*
plateau		MSWD = 4.6**	n=7	steps A-G	675.6	0.46		86.2	1.08	0.04*

Table 3. Argon isotopic results for furnace incremental heating analyses.

ID	Temp (°C)	$^{40}Ar/^{39}Ar$	$^{37}Ar/^{39}Ar$	$^{36}Ar/^{39}Ar$ (x 10^{-3})	$^{39}Ar_K$ (x 10^{-16} mol)	K/Ca	$^{40}Ar^*$ (%)	^{39}Ar (%)	Age (Ma)	±1σ (Ma)
01RB068, 167.07 mg groundmass concentrate, J=0.0001093, D=1.00712, NM-153, Lab#=53234-01										
A	650	1357.4	3.218	4528.4	36.7	0.16	1.4	6.5	3.9	1.6
B	730	32.59	0.8482	71.90	210.0	0.60	35.0	43.4	2.25	0.03
C	780	27.79	0.5376	54.36	46.7	0.95	42.3	51.7	2.32	0.04
D	830	30.31	0.5722	65.98	85.6	0.89	35.8	66.7	2.14	0.03
E	905	42.60	0.9548	106.9	78.9	0.53	26.0	80.6	2.18	0.04
F	1005	55.99	1.744	151.5	40.2	0.29	20.3	87.7	2.24	0.07
G	1105	96.37	2.685	289.6	25.1	0.19	11.4	92.1	2.17	0.13
H	1280	320.9	20.73	994.1	38.2	0.025	9.0	98.8	5.76	0.40
I	1700	955.3	27.04	3112.1	6.62	0.019	4.0	100.0	7.6	1.1
total gas age			n=9		568.0	0.55			2.63	0.36*
plateau		MSWD = 2.6**	n=7	steps A-G	523.2	0.60		92.1	2.22	0.05*
01RB043, 6.41 mg biotite, J=0.0014647, D=1.00698, NM-152, Lab#=53170-01										
A	650	257.4	0.0410	856.6	28.7	12.4	1.6	1.5	11.1	5.6
B	750	28.18	0.0247	71.32	52.6	20.7	25.2	4.4	18.67	0.67
C	850	11.20	0.0182	10.13	382.4	28.1	73.3	25.0	21.56	0.12
D	920	9.669	0.0195	4.702	477.6	26.1	85.6	50.8	21.75	0.08
E	1000	9.984	0.0413	6.018	431.7	12.3	82.2	74.0	21.56	0.09
F	1075	9.616	0.0322	4.842	264.6	15.8	85.1	88.3	21.51	0.08
G	1110	9.264	0.0553	3.191	146.1	9.2	89.9	96.2	21.87	0.10
H	1180	8.961	0.3769	2.550	53.5	1.4	91.9	99.1	21.64	0.16
I	1210	8.578	0.8072	1.902	13.6	0.63	94.2	99.8	21.24	0.36
J	1250	8.967	0.8284	2.231	2.92	0.62	93.4	99.9	22.0	1.0
L	1700	181.9	1.271	614.5	1.00	0.40	0.2	100.0	1.1	9.4
total gas age			n=11		1854.8	19.2			21.37	0.42*
plateau		MSWD = 1.8	n=8	steps C-J	1772.4	19.3		95.6	21.65	0.09*
01RB066, 6.74 mg biotite, J=0.0014633, D=1.00698, NM-152, Lab#=53169-01										
A	650	169.7	0.1721	564.7	9.11	3.0	1.7	0.5	7.4	4.4
B	750	15.25	0.0812	25.74	13.7	6.3	50.1	1.3	20.07	0.57
C	850	9.818	0.0447	5.258	158.2	11.4	84.2	10.4	21.70	0.10
D	920	8.387	0.0157	1.570	302.7	32.5	94.5	27.7	20.80	0.06
E	1000	8.298	0.0205	1.344	360.9	24.9	95.2	48.3	20.74	0.06
F	1075	8.678	0.0291	2.990	315.4	17.5	89.8	66.4	20.47	0.07
G	1110	8.631	0.0333	2.462	218.1	15.3	91.6	78.9	20.75	0.08
H	1180	8.365	0.1479	1.582	150.4	3.5	94.6	87.5	20.76	0.11
I	1210	8.128	0.0681	0.7864	218.5	7.5	97.2	100.0	20.74	0.07
total gas age			n=9		1747.1	18.2			20.72	0.20*
plateau		MSWD = 2.9**	n=6	steps D-I	1566.1	19.1		89.6	20.71	0.10*
01RB062, 8.60 mg biotite, J=0.0014668, D=1.00698, NM-152, Lab#=53171-01										
A	650	333.1	0.0739	1107.9	45.0	6.9	1.7	2.1	15.0	6.5
B	750	29.84	0.1096	80.26	83.8	4.7	20.6	6.1	16.16	0.58
C	850	12.67	0.0629	16.78	227.9	8.1	60.9	16.8	20.31	0.17
D	920	10.81	0.0413	9.440	336.2	12.4	74.2	32.6	21.11	0.11
E	1000	9.973	0.0315	7.454	454.6	16.2	77.9	53.9	20.45	0.09
F	1075	9.881	0.0407	7.044	364.3	12.5	79.0	71.1	20.53	0.10
G	1110	9.139	0.0838	4.383	182.8	6.1	85.9	79.7	20.66	0.09
H	1180	8.600	0.1449	2.699	232.8	3.5	90.9	90.6	20.56	0.07
I	1210	8.359	0.2528	2.060	152.5	2.0	93.0	97.8	20.45	0.08
J	1250	8.367	0.1628	2.225	47.0	3.1	92.3	100.0	20.32	0.14
K	1300	73.81	10.29	86.14	0.100	0.050	66.7	100.0	127	43
L	1700	595.5	5.214	2013.8	0.336	0.098	0.1	100.0	2	29
total gas age			n=12		2127.4	9.9			20.30	0.52*
plateau		MSWD = 1.2	n=6	steps E-J	1434.1	10.0		67.4	20.51	0.08*

Table 3. Argon isotopic results for furnace incremental heating analyses.

ID	Temp (°C)	$^{40}Ar/^{39}Ar$	$^{37}Ar/^{39}Ar$	$^{36}Ar/^{39}Ar$ (x 10^{-3})	$^{39}Ar_K$ (x 10^{-16} mol)	K/Ca	$^{40}Ar^*$ (%)	^{39}Ar (%)	Age (Ma)	±1σ (Ma)
01RB062, 24.18 mg hornblende, J=0.0014621, D=1.00698, NM-152, Lab#=53168-01										
A	800	101.4	1.242	312.3	26.3	0.41	9.1	3.6	24.2	2.5
B	900	15.56	0.7677	24.55	23.7	0.66	53.8	6.9	21.95	0.44
C	1000	13.00	0.9375	16.89	30.0	0.54	62.2	11.0	21.21	0.33
D	1030	10.69	1.693	9.411	14.7	0.30	75.3	13.0	21.14	0.35
E	1060	9.925	2.466	7.821	15.9	0.21	78.8	15.2	20.54	0.39
F	1090	11.16	5.728	12.08	30.3	0.089	72.3	19.3	21.23	0.20
G	1120	12.21	6.884	14.53	111.4	0.074	69.5	34.6	22.35	0.18
H	1170	8.963	5.542	4.772	380.5	0.092	89.4	86.7	21.09	0.08
I	1200	8.848	5.155	4.387	57.2	0.099	90.2	94.6	21.00	0.17
J	1250	9.735	6.850	6.583	33.3	0.074	85.8	99.1	22.02	0.27
K	1300	11.82	7.331	14.81	4.49	0.070	68.1	99.7	21.2	1.2
L	1700	113.4	16.28	360.5	1.89	0.031	7.2	100.0	21.8	5.6
total gas age			n=12		729.9	0.14			21.46	0.52*
plateau		MSWD = 0.25	n=2	steps H-I	437.7	0.09		60.0	21.07	0.15*
SRD-0101, 12.75 mg biotite, J=0.0014554, D=1.00698, NM-152, Lab#=53151-01										
A	650	899.4	0.7016	3003.3	38.3	0.73	1.3	1.1	31	18
B	750	227.9	0.9999	732.9	88.4	0.51	5.0	3.6	29.6	4.3
C	850	68.84	0.0199	210.1	252.2	25.7	9.8	10.7	17.6	1.3
D	920	18.16	0.0166	33.69	422.5	30.7	45.2	22.7	21.42	0.27
E	1000	11.24	0.0077	10.96	1242.2	66.4	71.2	57.8	20.90	0.12
F	1075	10.97	0.0108	10.61	802.6	47.2	71.4	80.5	20.46	0.11
G	1110	9.620	0.0263	5.384	316.9	19.4	83.5	89.5	20.96	0.09
H	1180	9.346	0.1133	4.043	160.7	4.5	87.3	94.0	21.30	0.10
I	1210	9.037	0.1414	2.380	81.3	3.6	92.3	96.3	21.78	0.11
J	1250	8.929	0.1912	1.961	64.9	2.7	93.7	98.2	21.83	0.12
K	1300	8.755	0.0883	0.8747	41.9	5.8	97.1	99.4	22.19	0.17
L	1700	12.05	0.8420	10.89	22.3	0.61	73.9	100.0	23.23	0.35
total gas age			n=12		3534.2	41.8			21.1	1.1*
plateau		MSWD = 8.9**	n=5	steps D-H	2944.9	47.6		83.3	20.93	0.33*
VY122001-3, 195.51 mg groundmass concentrate, J=0.000112, D=1.00712, NM-153, Lab#=53260-01										
A	650	1501.3	0.7846	5025.3	37.5	0.65	1.1	7.8	3.3	1.7
B	730	49.70	1.351	150.3	197.9	0.38	10.9	48.7	1.09	0.06
C	780	48.41	2.359	152.2	64.3	0.22	7.5	62.0	0.74	0.07
D	830	44.70	2.549	140.7	70.7	0.20	7.4	76.6	0.67	0.06
E	905	54.30	2.684	171.8	48.8	0.19	6.9	86.7	0.76	0.07
F	1005	105.0	3.858	340.5	24.8	0.13	4.5	91.9	0.95	0.14
G	1105	263.8	6.424	874.5	10.9	0.079	2.2	94.1	1.20	0.38
H	1280	145.0	29.78	471.6	22.9	0.017	5.6	98.9	1.67	0.19
I	1700	628.2	20.46	2066.9	5.52	0.025	3.0	100.0	3.92	0.82
total gas age			n=9		483.4	0.29			1.18	0.44*
plateau		MSWD =1.2	n=5	steps C-G	219.5	0.19		45.4	0.74	0.07*
VY122001-9, 188.96 mg groundmass concentrate, J=0.0001082, D=1.00712, NM-153, Lab#=53228-01										
B	700	118.1	0.4063	392.6	84.0	1.3	1.8	11.9	0.41	0.13
C	750	75.42	0.3358	266.2	0.629	1.5	-4.2	12.0	-0.63	0.68
D	800	37.18	0.8836	116.3	122.8	0.58	7.7	29.4	0.56	0.05
E	875	30.45	1.080	90.08	112.3	0.47	12.9	45.3	0.76	0.04
F	1000	21.54	1.071	60.93	246.8	0.48	16.8	80.2	0.71	0.02
G	1110	61.51	1.322	191.9	82.6	0.39	8.0	91.9	0.96	0.07
H	1280	117.0	5.888	373.5	44.7	0.087	6.1	98.3	1.39	0.13
I	1700	214.7	12.63	709.5	12.2	0.040	2.9	100.0	1.21	0.31
total gas age			n=8		706.0	0.54			0.74	0.12*

Table 3. Argon isotopic results for furnace incremental heating analyses.

ID	Temp (°C)	$^{40}Ar/^{39}Ar$	$^{37}Ar/^{39}Ar$	$^{36}Ar/^{39}Ar$ (x 10^{-3})	$^{39}Ar_K$ (x 10^{-16} mol)	K/Ca	^{40}Ar* (%)	^{39}Ar (%)	Age (Ma)	±1σ (Ma)
VY11802-7, 36.74 mg hornblende, J=0.0014688, D=1.00698, NM-152, Lab#=53173-01										
A	*800*	*52.61*	*0.6438*	*172.4*	*43.8*	*0.79*	*3.3*	*5.1*	*4.6*	*1.2*
B	*900*	*8.758*	*0.8164*	*27.56*	*36.4*	*0.62*	*7.8*	*9.4*	*1.80*	*0.38*
C	*1000*	*17.38*	*1.295*	*57.85*	*18.1*	*0.39*	*2.3*	*11.5*	*1.05*	*0.71*
D	*1030*	*24.85*	*1.348*	*81.46*	*8.38*	*0.38*	*3.6*	*12.5*	*2.4*	*1.2*
E	*1060*	*18.38*	*2.353*	*61.76*	*8.88*	*0.22*	*1.8*	*13.6*	*0.9*	*1.2*
F	*1090*	*6.450*	*4.691*	*19.71*	*27.6*	*0.11*	*15.7*	*16.8*	*2.69*	*0.35*
G	*1120*	*4.286*	*5.796*	*12.35*	*60.7*	*0.088*	*26.1*	*23.9*	*2.97*	*0.16*
H	1170	1.398	6.774	4.358	521.0	0.075	48.0	85.0	1.79	0.05
I	1200	1.331	6.902	4.290	82.3	0.074	47.7	94.7	1.69	0.11
J	*1250*	*1.845*	*8.489*	*6.888*	*43.8*	*0.060*	*27.7*	*99.8*	*1.36*	*0.14*
K	*1300*	*12.15*	*95.61*	*59.36*	*1.09*	*0.005*	*20.8*	*99.9*	*7.1*	*3.3*
L	*1700*	*412.8*	*338.1*	*1423.2*	*0.427*	*0.002*	*4.9*	*100.0*	*69*	*26*
total gas age			n=12		852.5	0.15			2.03	0.42*
plateau		MSWD = 0.67	n=2	steps H-I	603.4	0.08		70.8	1.77	0.09*

Notes:
Isotopic ratios corrected for blank, radioactive decay, and mass discrimination, not corrected for interferring reactions.
Individual analyses show analytical error only; plateau and total gas age errors include error in J and irradiation parameters.
n= number of heating steps
D= mass spectrometer discrmination
K/Ca = molar ratio calculated from reactor produced $^{39}Ar_K$ and $^{37}Ar_{Ca}$.
* 2σ error
** MSWD outside 95% confidence interval

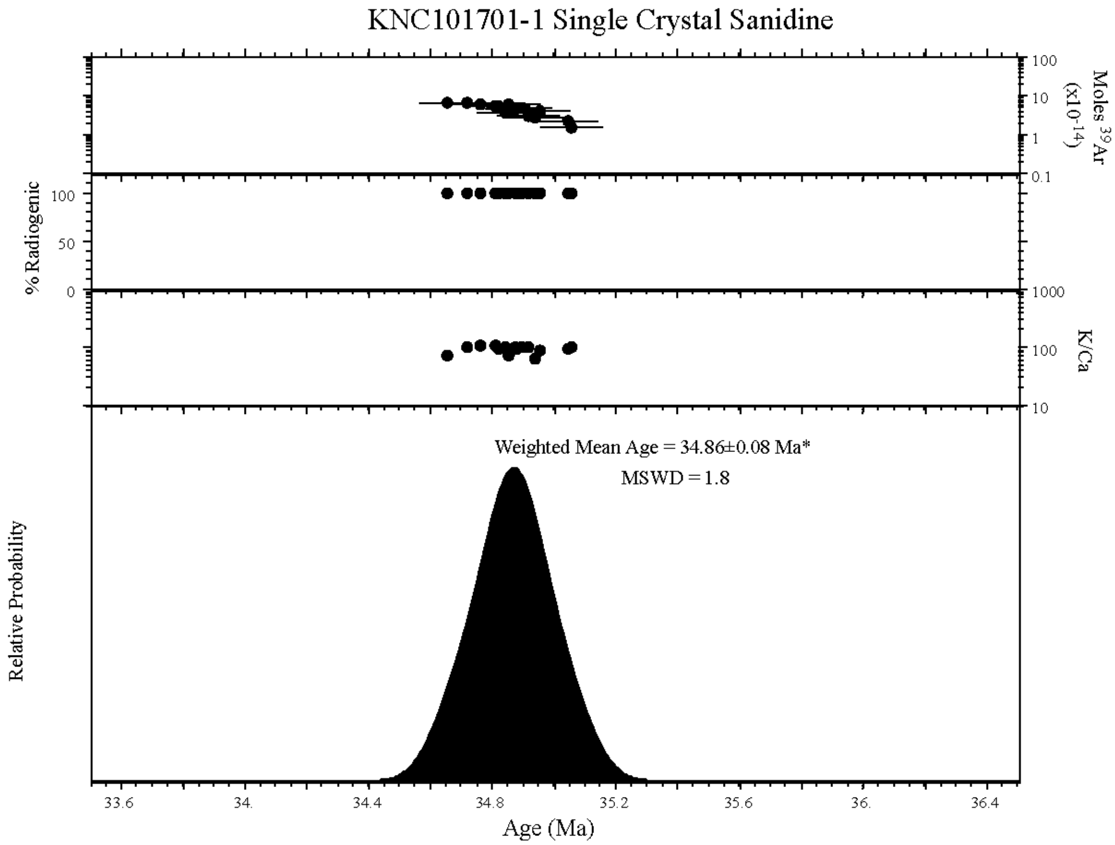

Figure 1. Age probability distribution diagram of single crystal sanidine from sample KNC101701-1. * 2σ

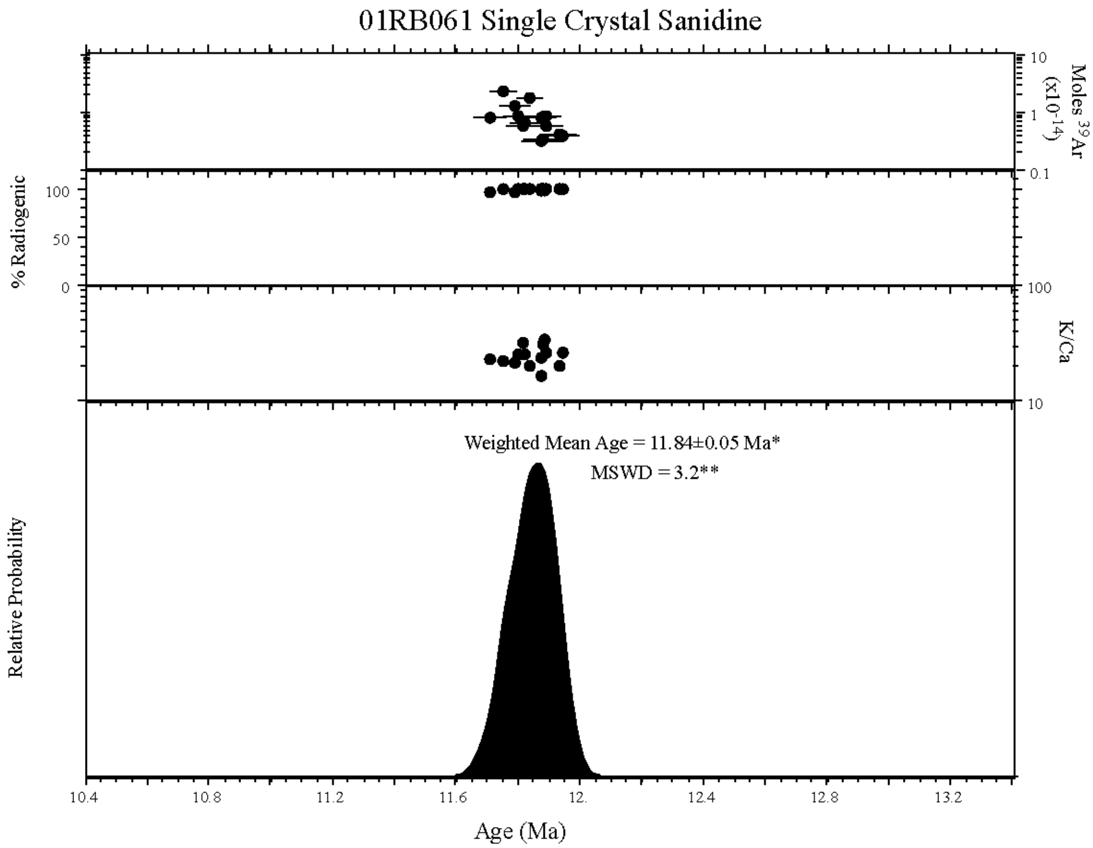

Figure 2. Age probability distribution diagram of single crystal sanidine from sample 01RB061. * 2σ ** outside 95% confidence interval

01RB067 Single Crystal Sanidine

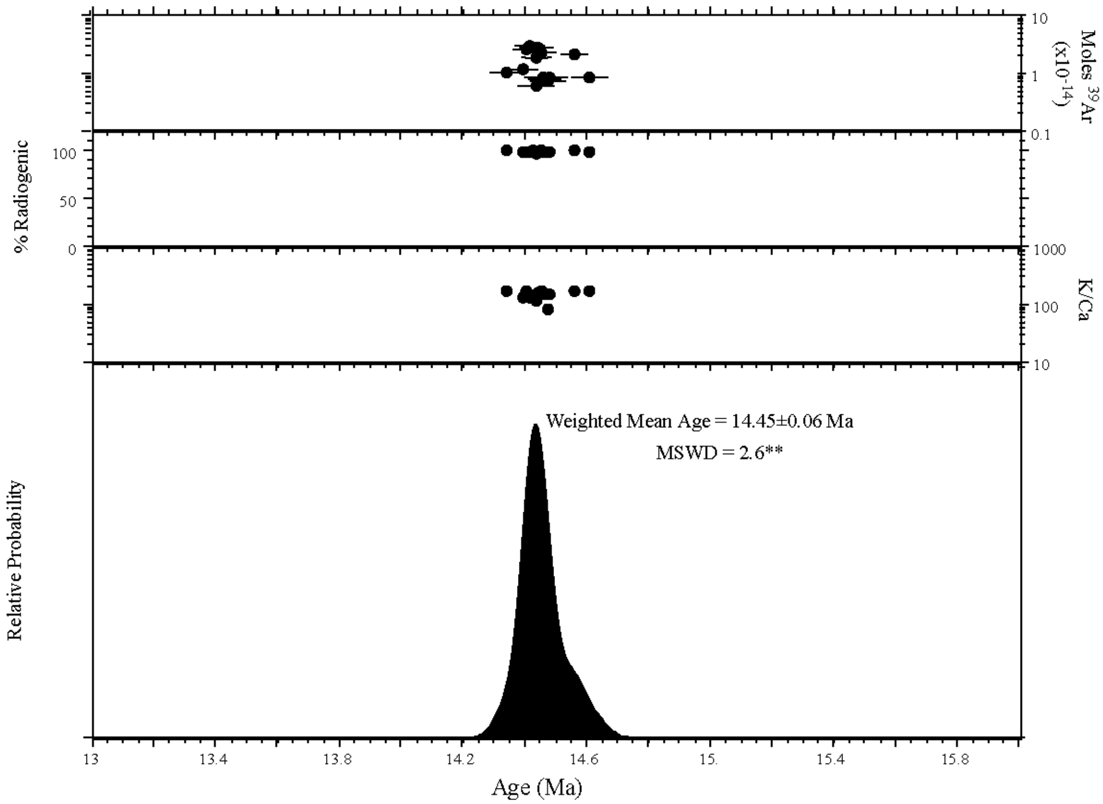

Figure 3. Age probability distribution diagram of single crystal sanidine from sample 01RB067. * 2σ ** outside 95% confidence interval

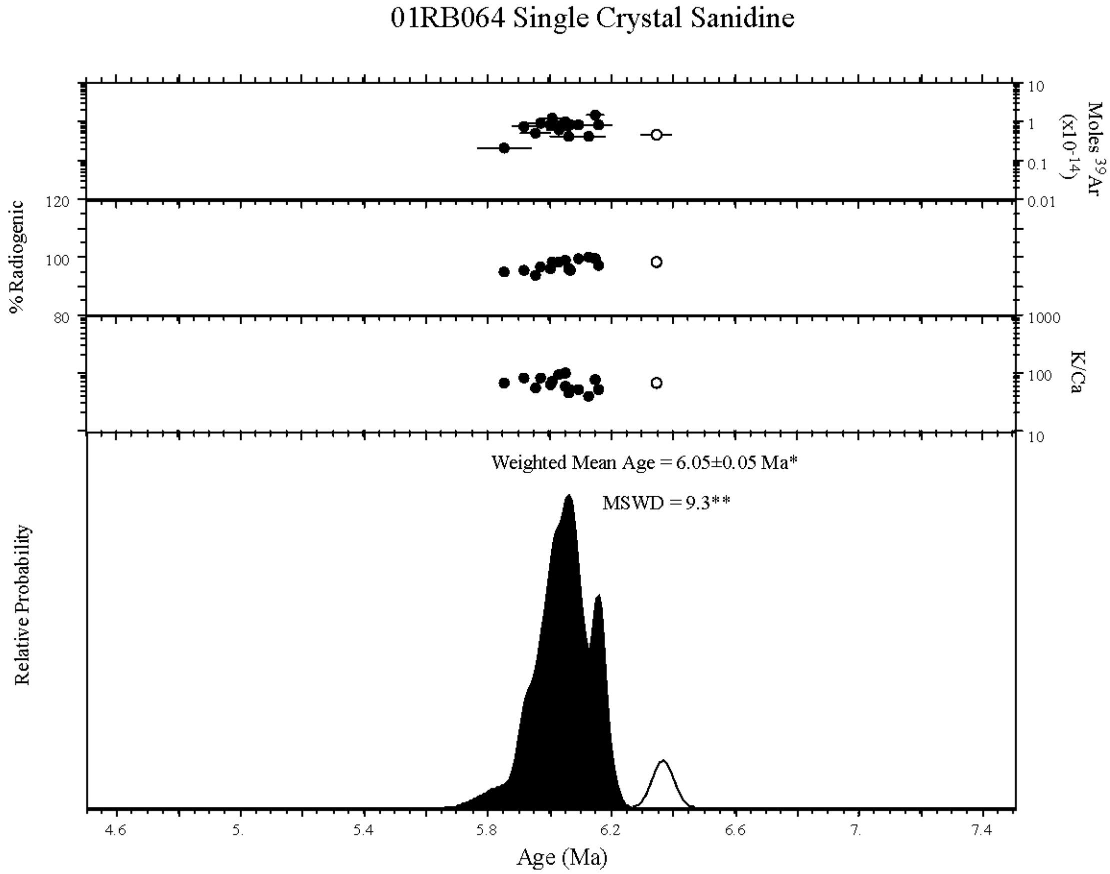

Figure 4. Age probability distribution diagram of single crystal sanidine from sample 01RB064. * 2σ ** outside 95% confidence interval

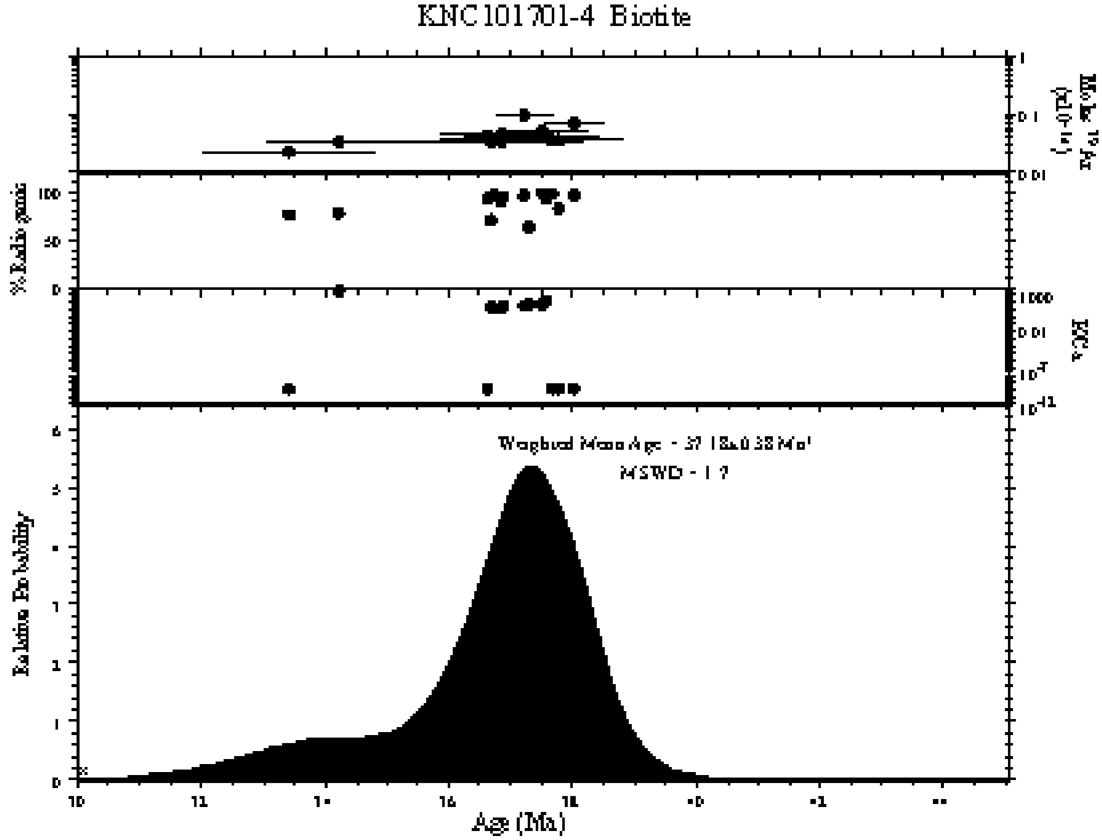

Figure 5. Age probability distribution diagram of single crystal biotite from sample KNC101701-4. * 2σ

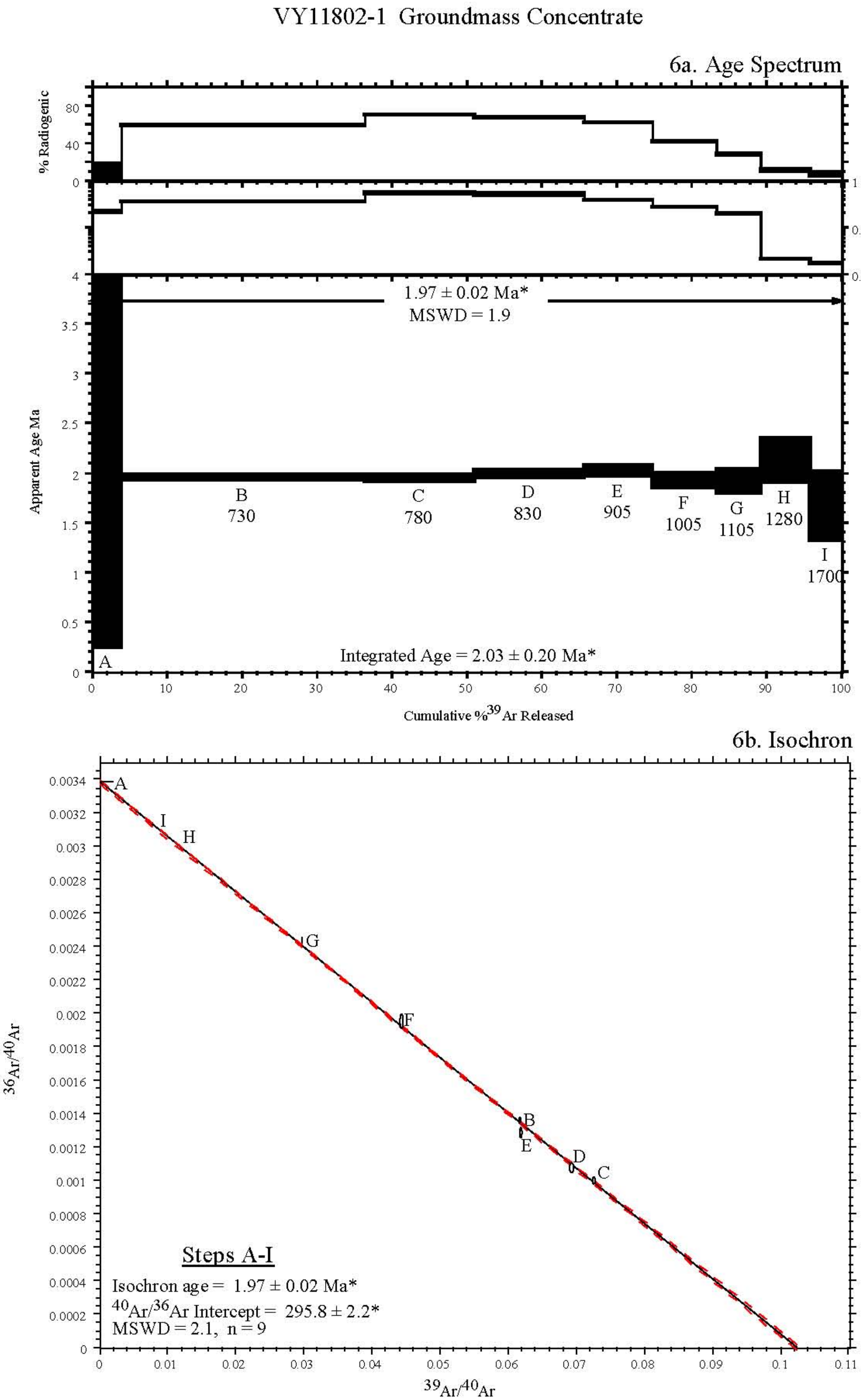

Figure 6. Age spectrum (6a) and isochron (6b) for sample VY11802-1 groundmass concentrate.
*2σ **outside 95% confidence interval

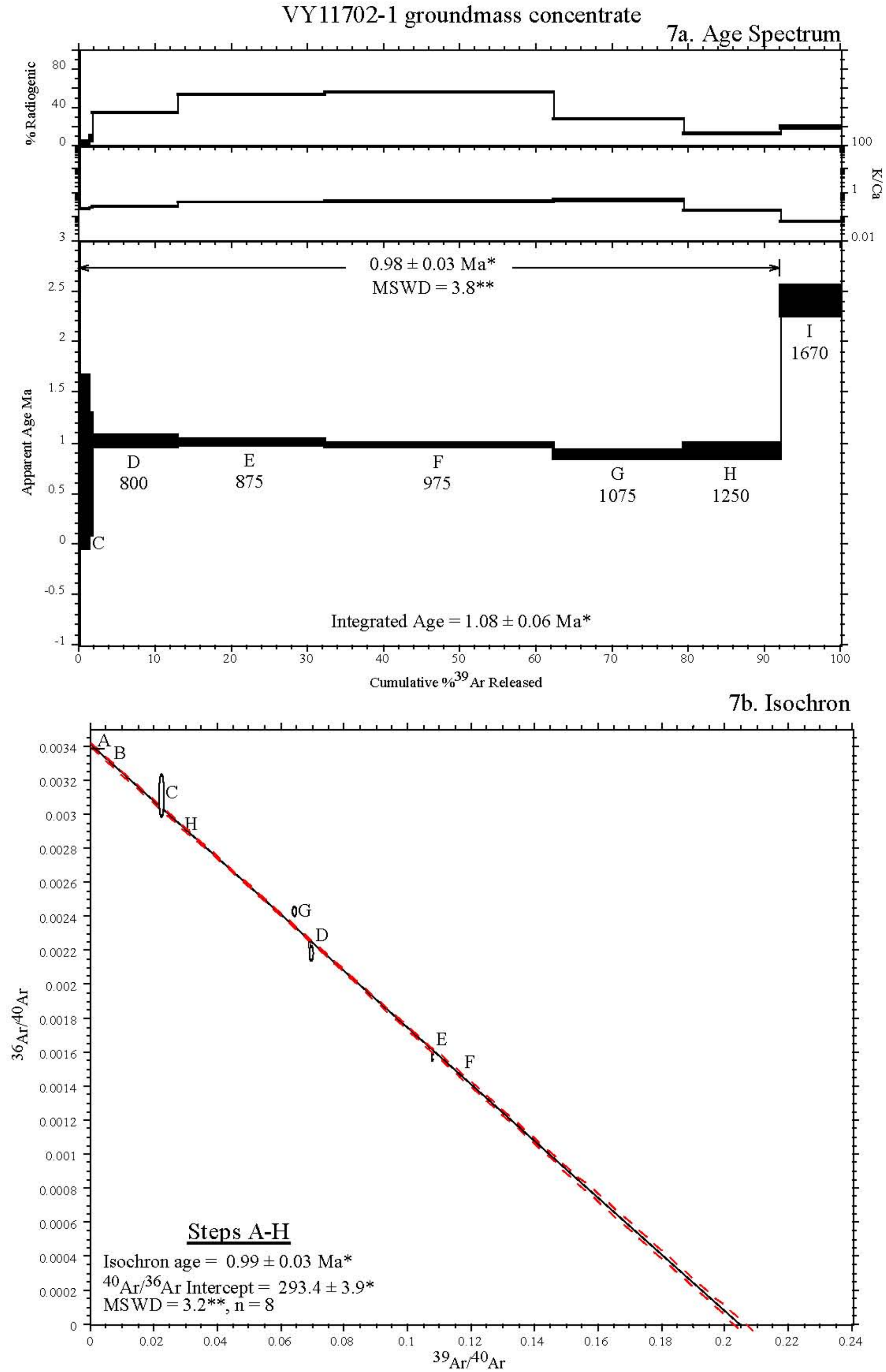

Figure 7. Age spectrum (7a) and isochron (7b) for sample VY11702-1 groundmass concentrate.
*2σ **outside 95% confidence interval

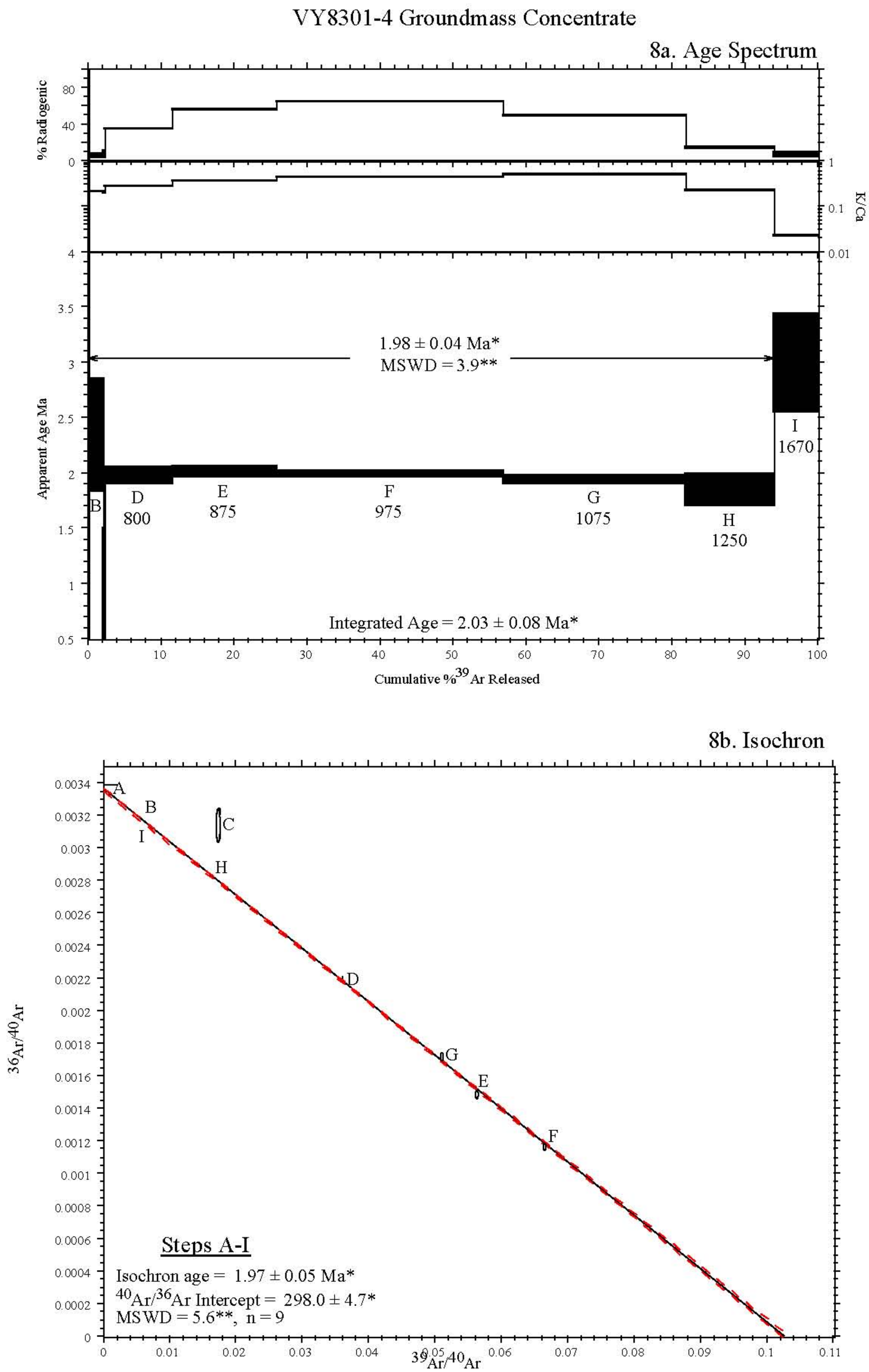

Figure 8. Age spectrum (8a) and isochron (8b) for sample VY8301-4 groundmass concentrate.
*2σ **outside 95% confidence interval

VY8301-9 Groundmass Concentrate

9a. Age Spectrum

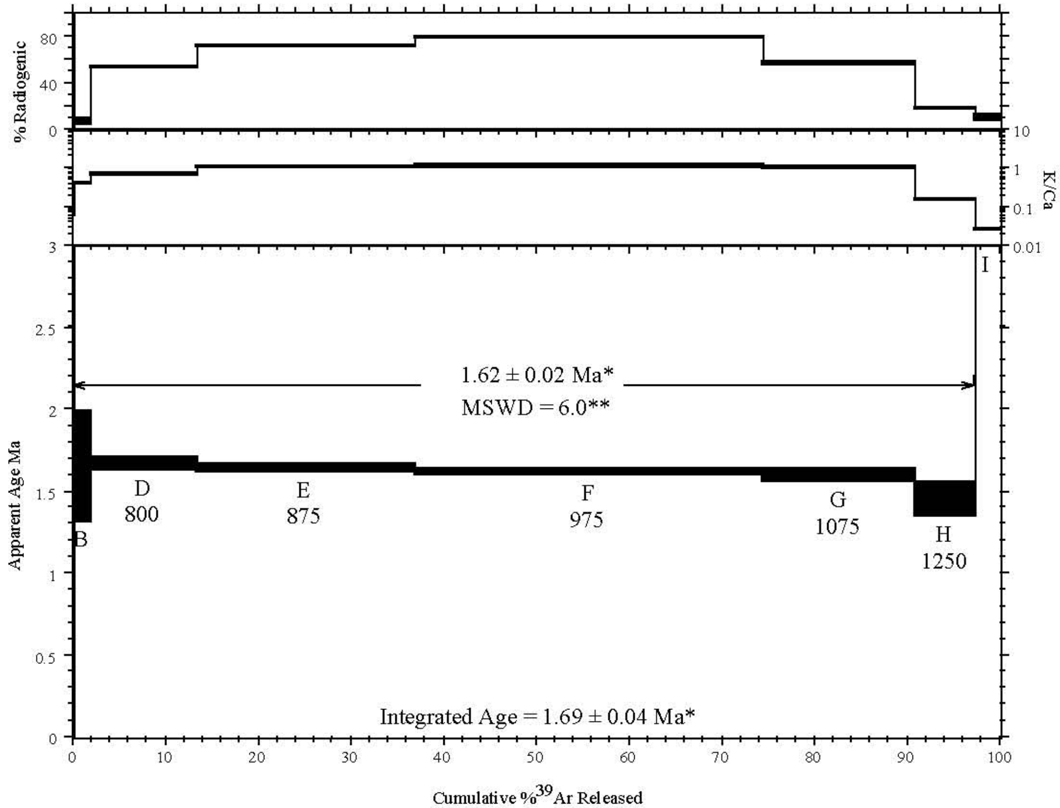

9b. Isochron

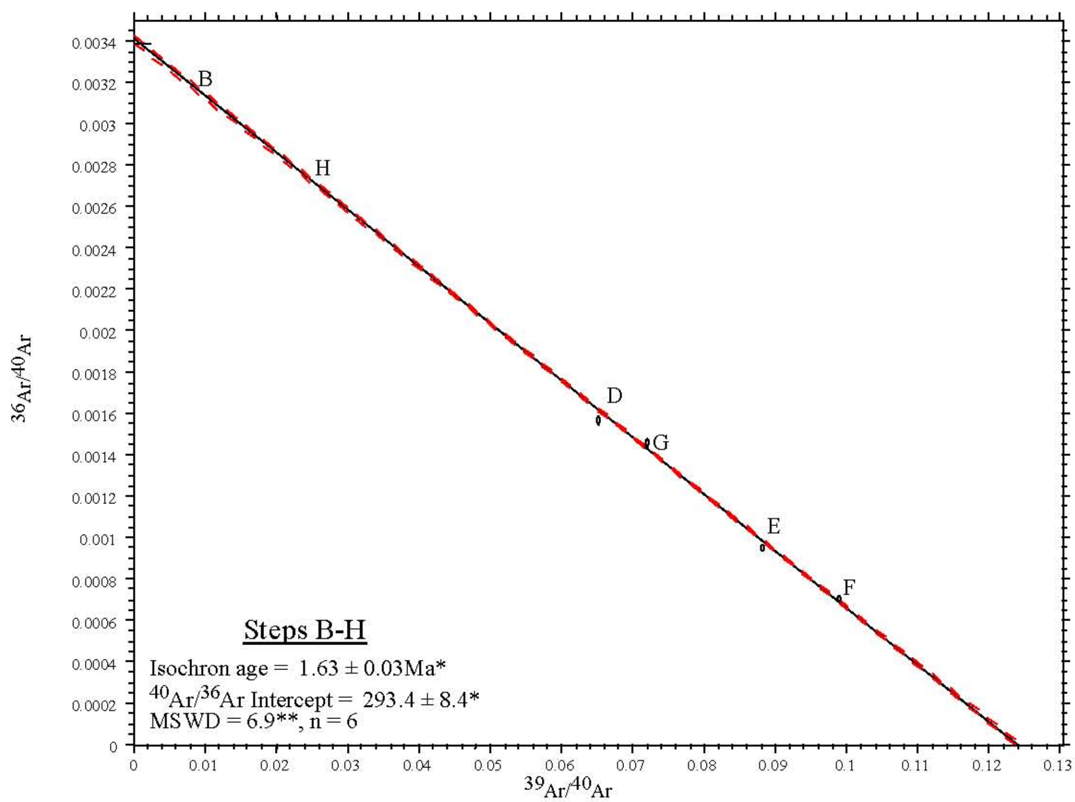

Figure 9. Age spectrum (9a) and isochron (9b) for sample VY8301-9 groundmass concentrate.
*2σ **outside 95% confidence interval

VY122001-1 Groundmass Concentrate

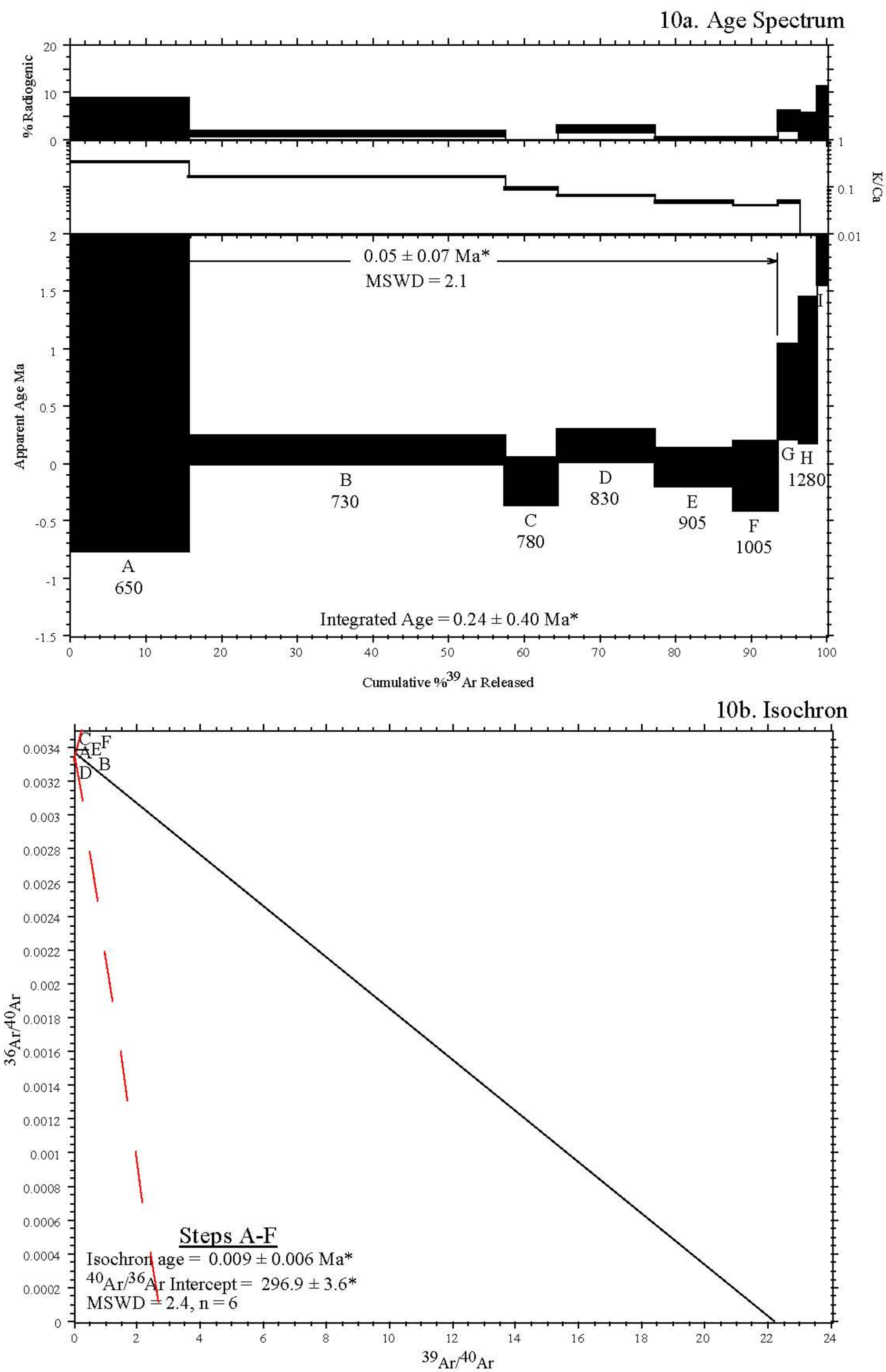

Figure 10. Age spectrum (10a) and isochron (10b) for sample VY122001-1 groundmass concentrate.
*2σ **outside 95% confidence interval

VY122001-4 Groundmass Concentrate

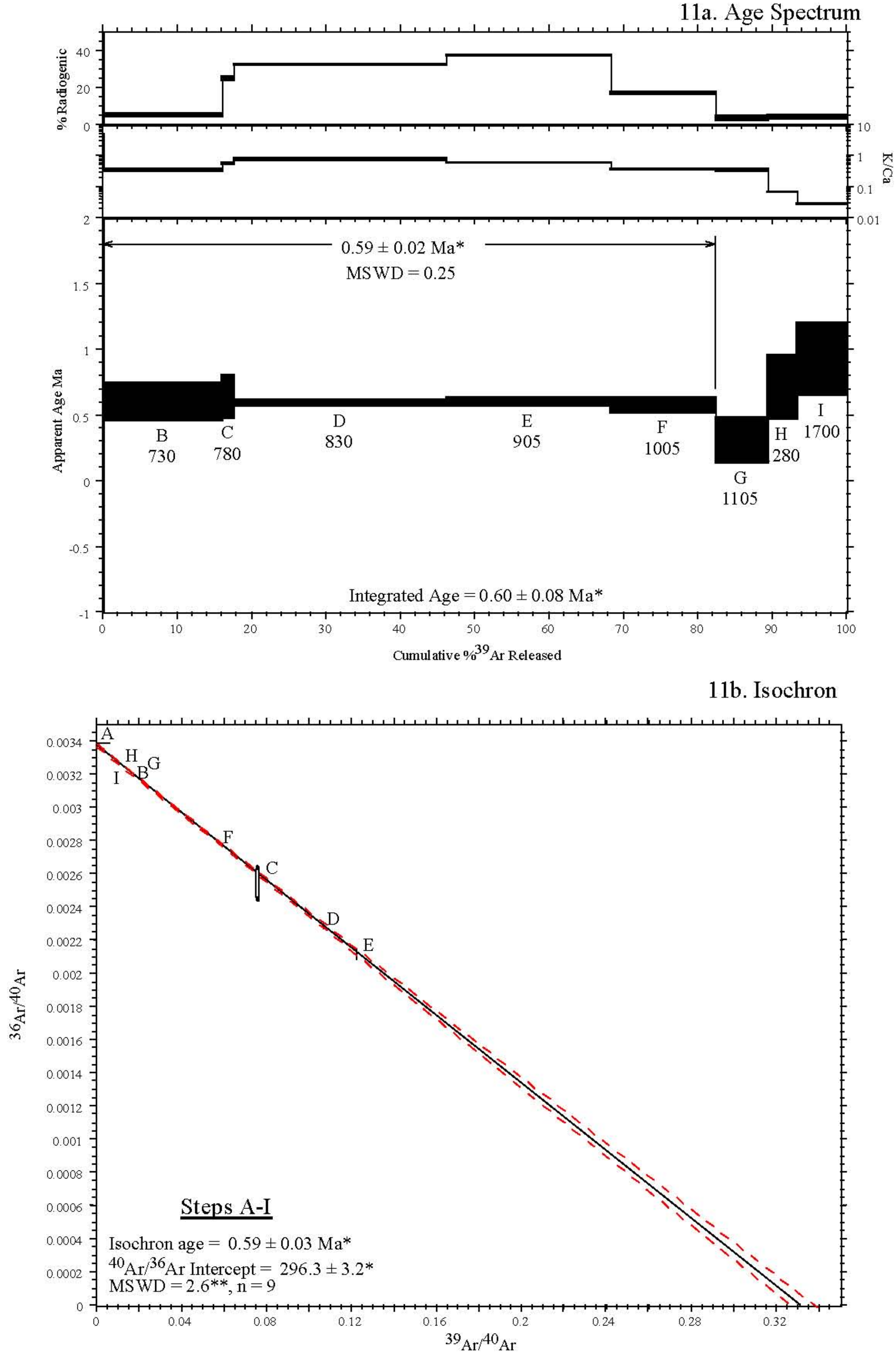

Figure 11. Age spectrum (11a) and isochron (11b) for sample VY122001-4 groundmass concentrate.
*2σ **outside 95% confidence interval

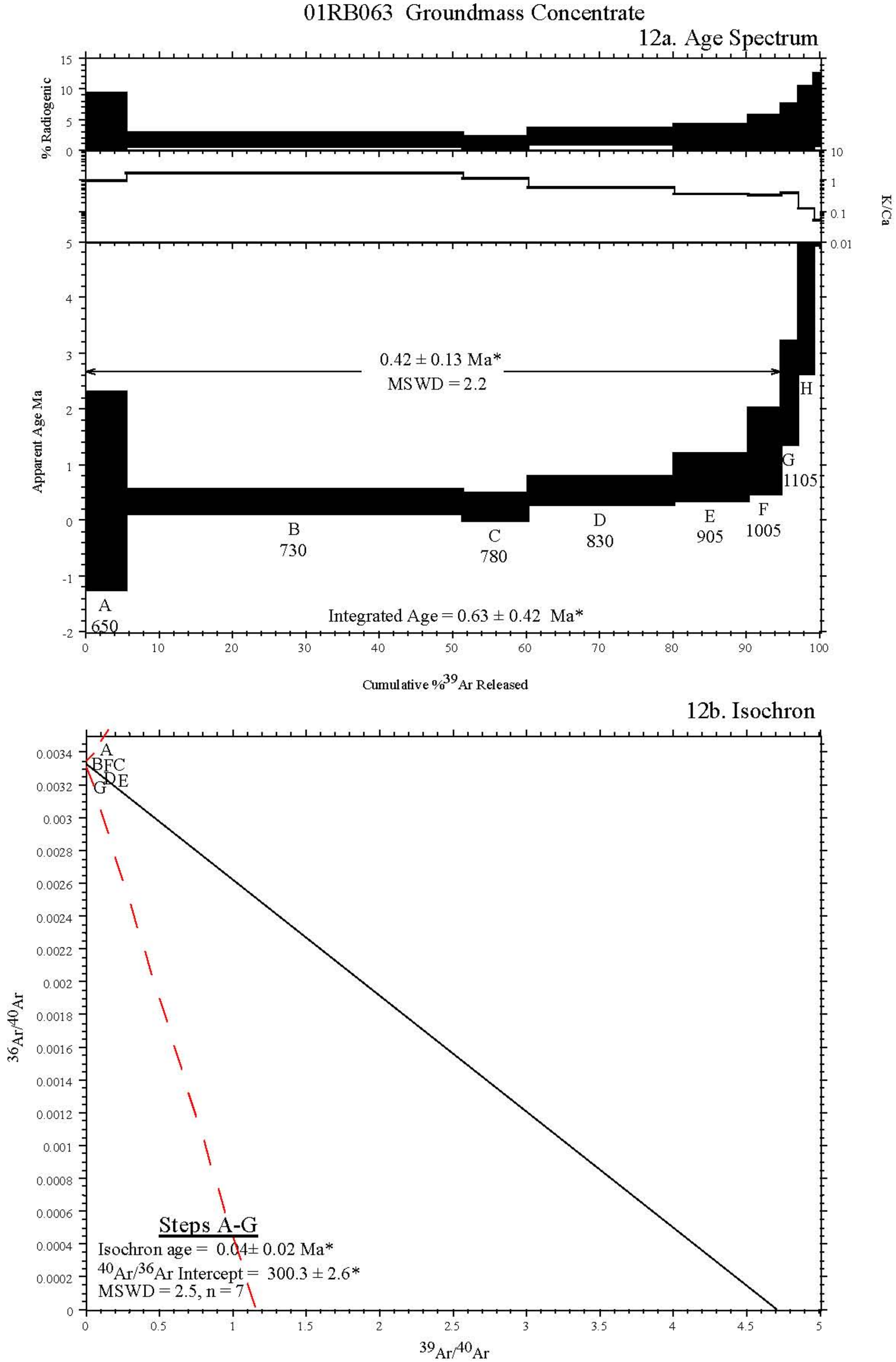

Figure 12. Age spectrum (12a) and isochron (12b) for sample 01RB063 groundmass concentrate.
*2σ **outside 95% confidence interval

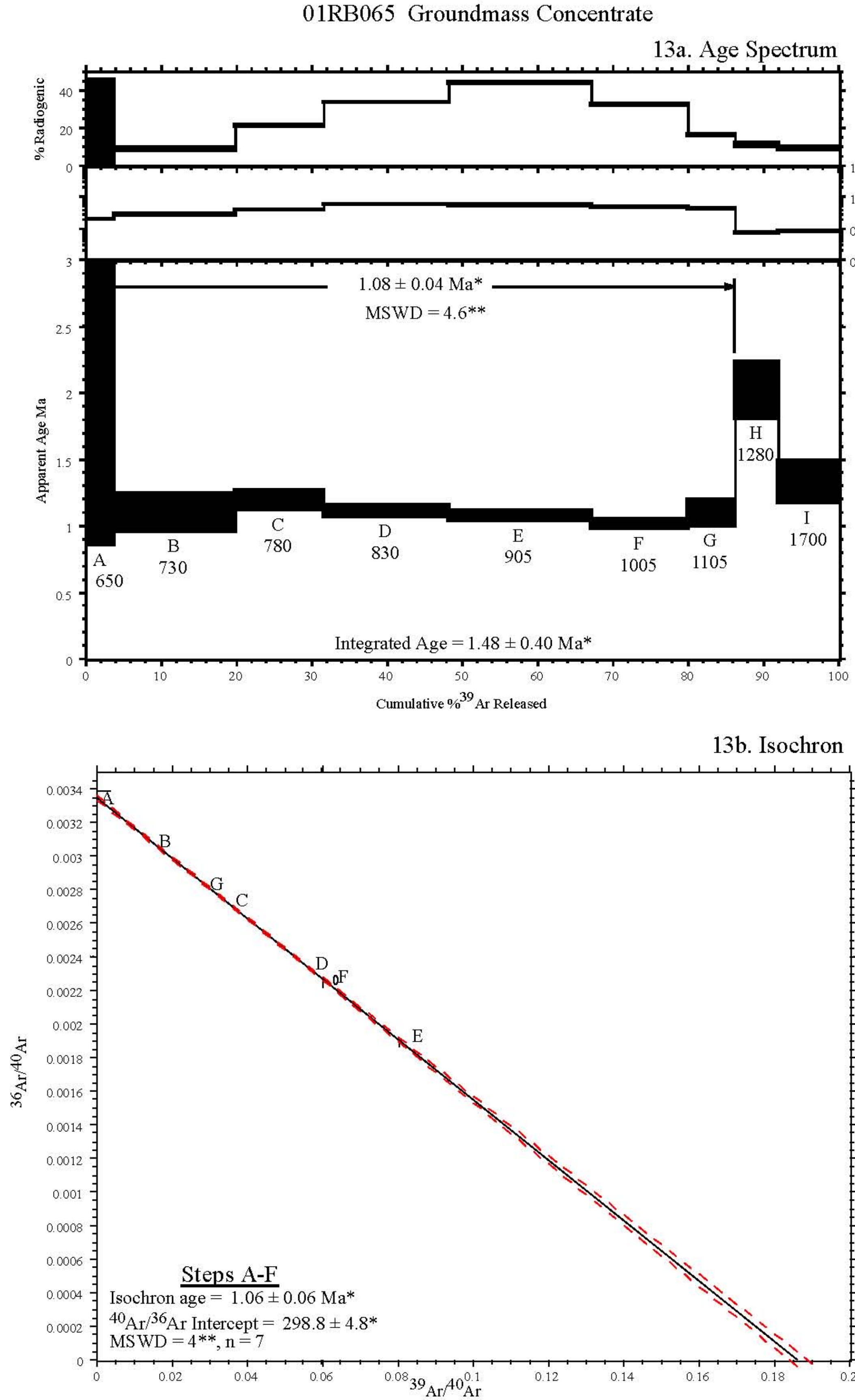

Figure 13. Age spectrum (13a) and isochron (13b) for sample 01RB065 groundmass concentrate.
*2σ **outside 95% confidence interval

01RB068 Groundmass Concentrate

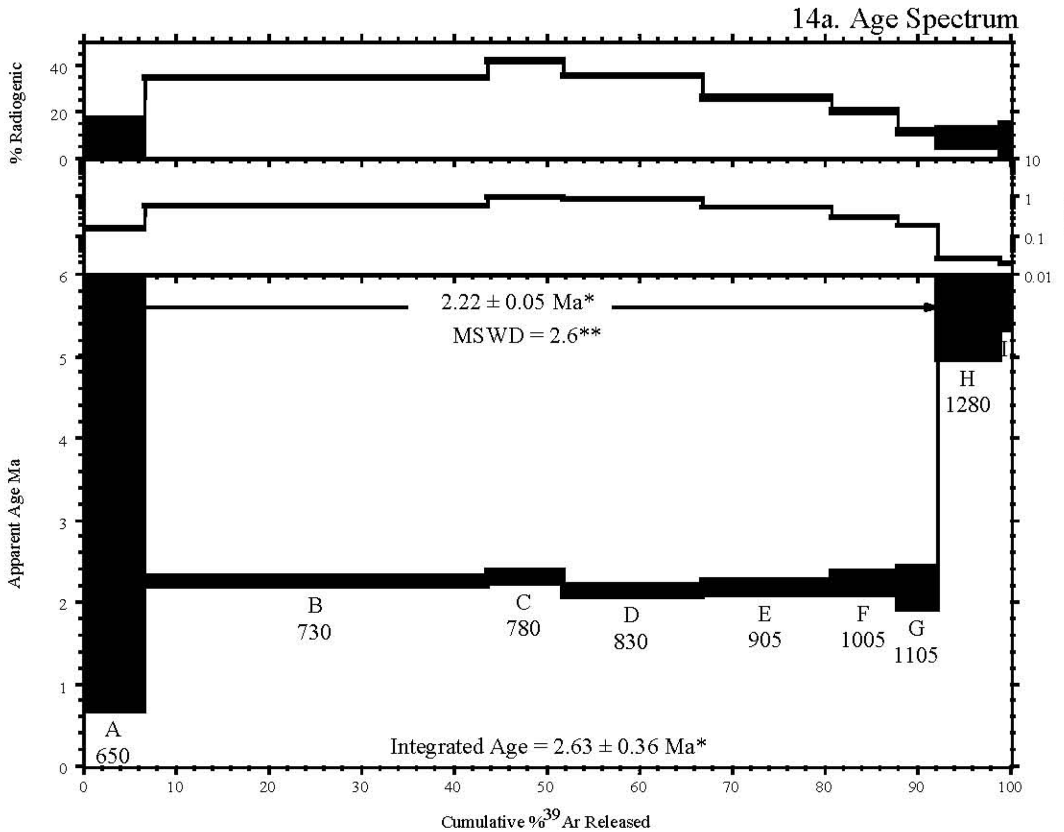

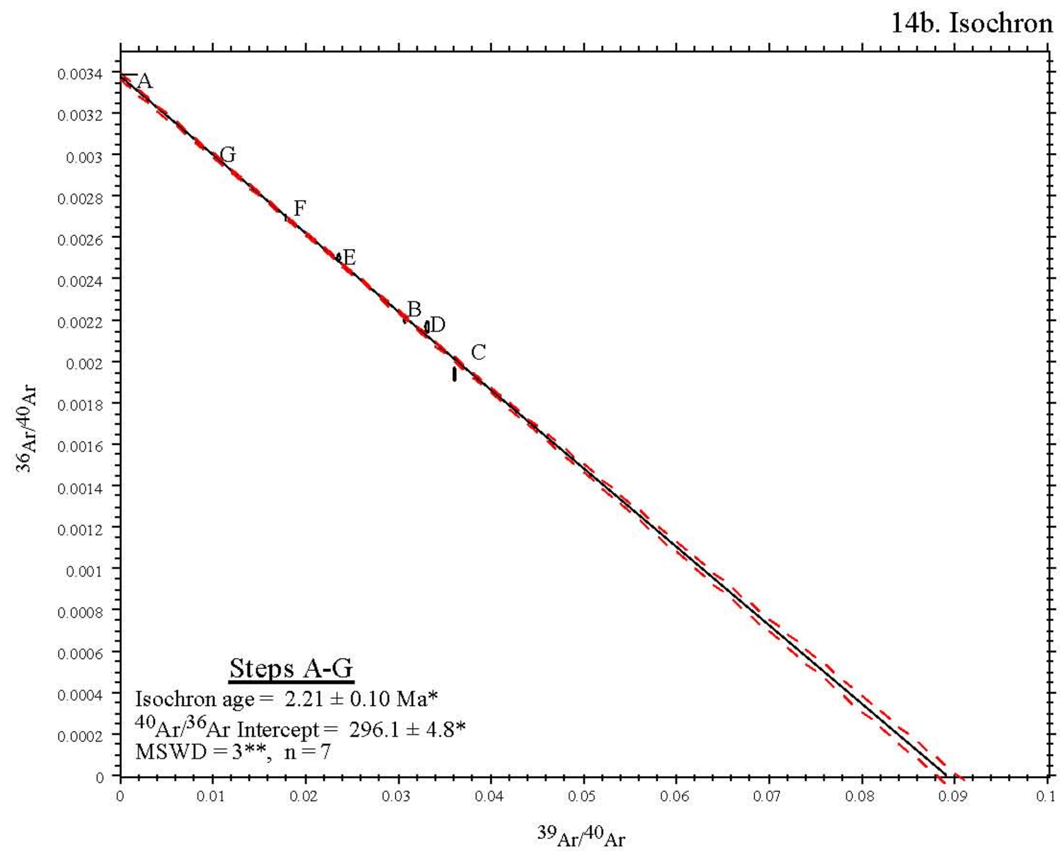

Figure 14. Age spectrum (14a) and isochron (14b) for sample 01RB068 groundmass concentrate. *2σ **outside 95% confidence interval

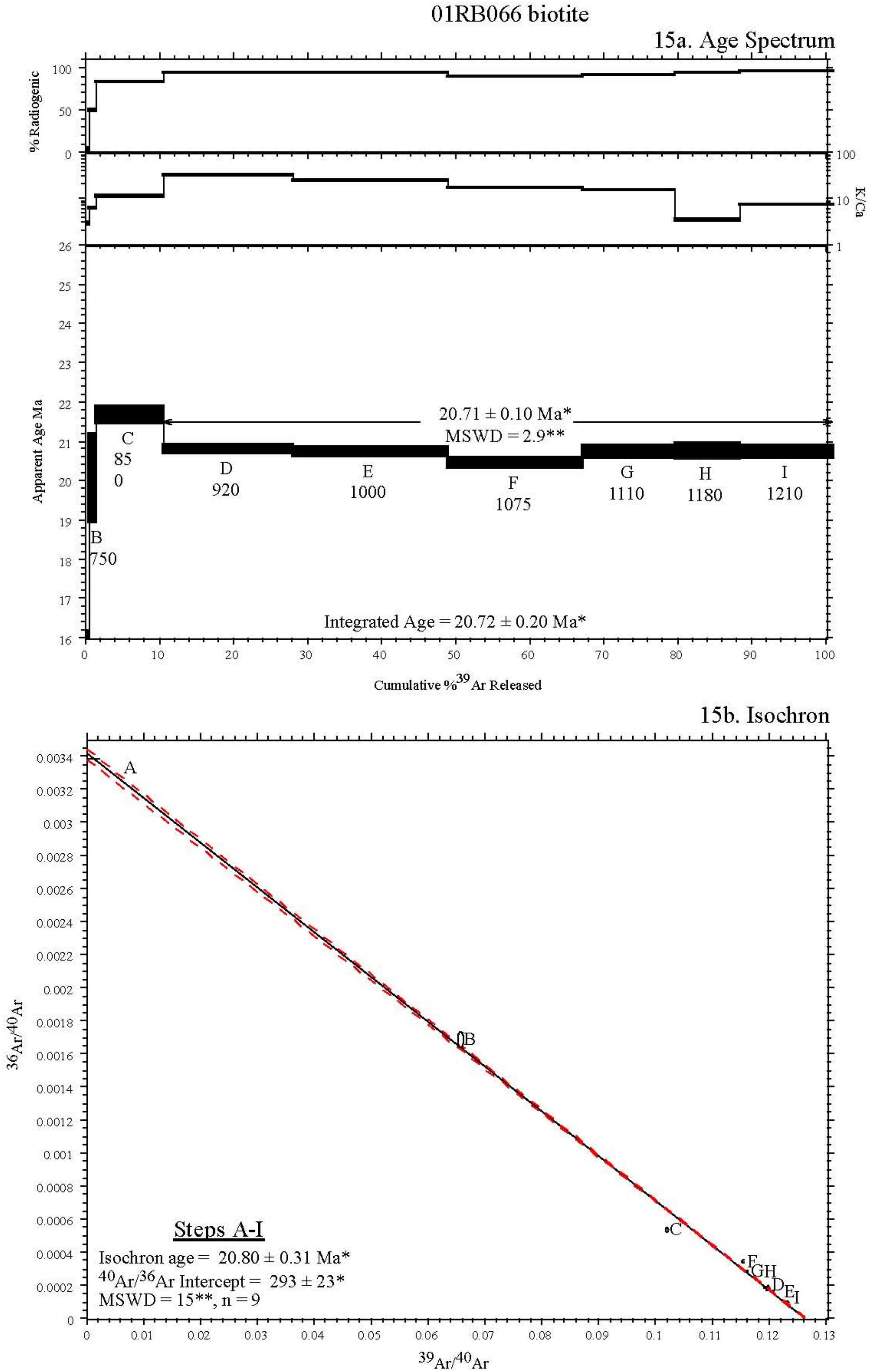

Figure 15. Age spectrum (15a) and isochron (15b) for sample 01RB066 biotite.
*2σ **outside 95% confidence interval

01RB043 Biotite

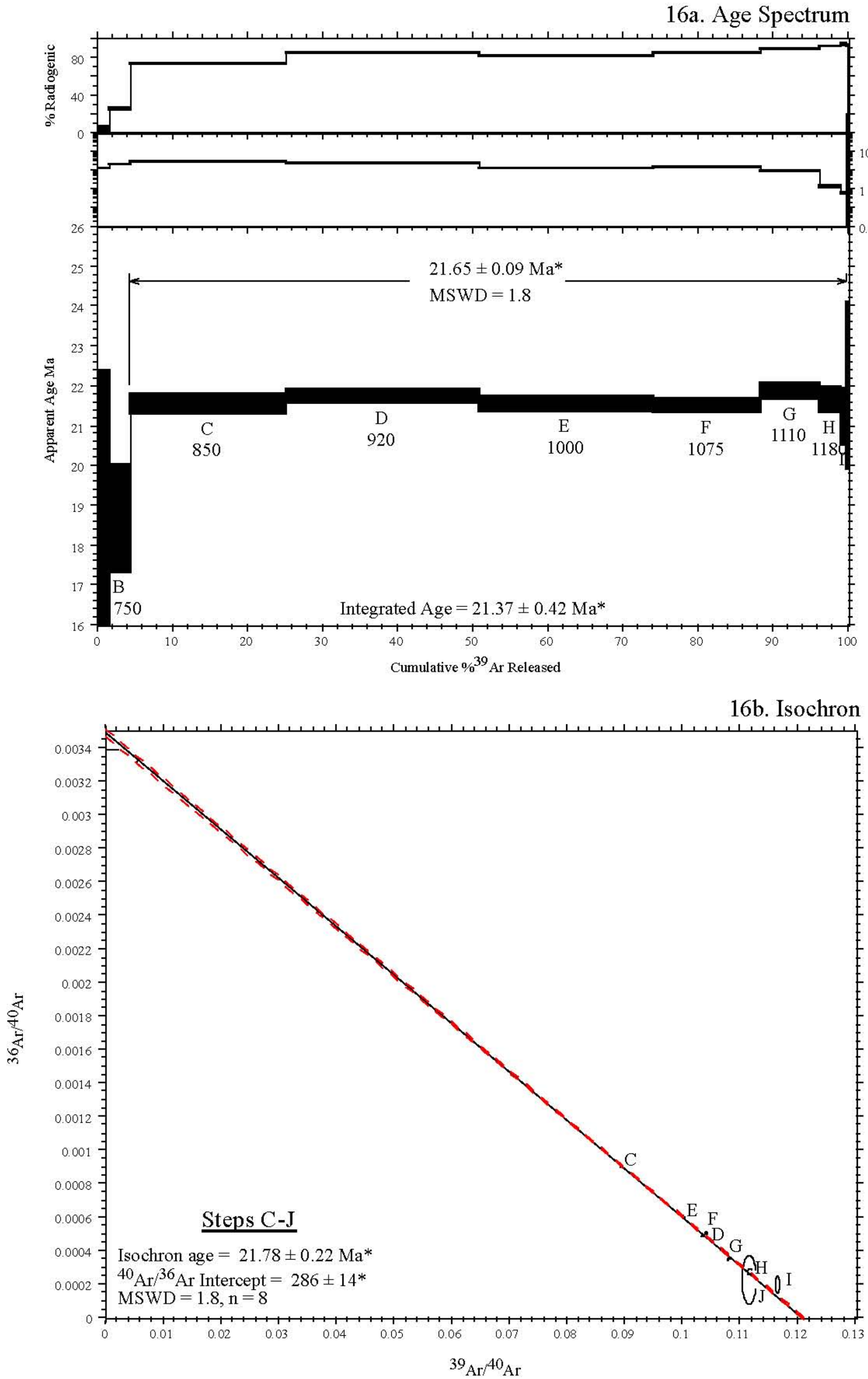

Figure 16. Age spectrum (16a) and isochron (16b) for sample 01RB043 biotite.
*2σ **outside 95% confidence interval

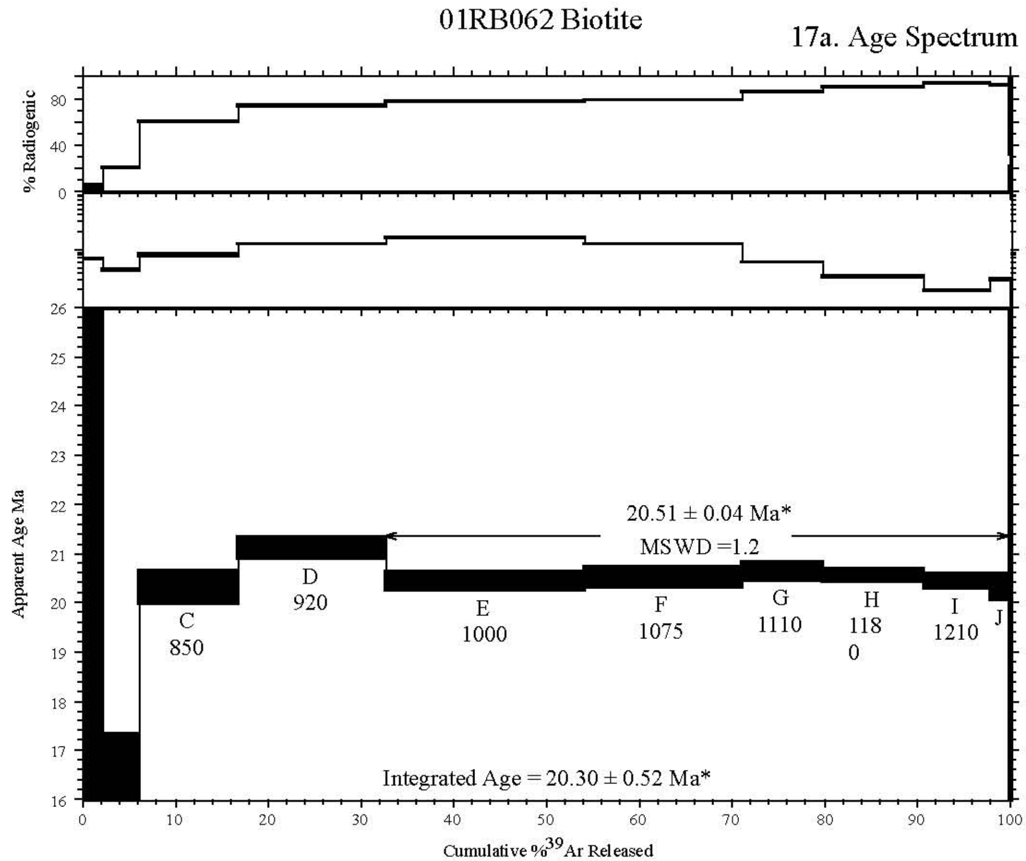

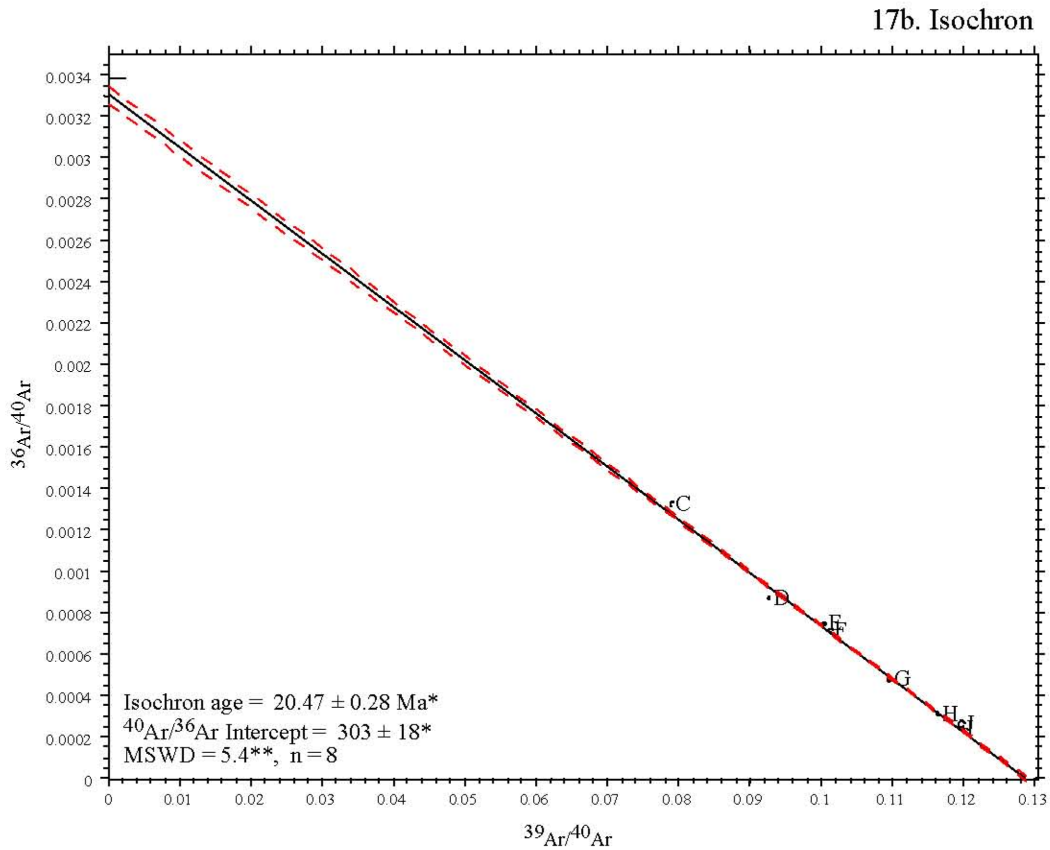

Figure 17. Age spectrum (17a) and isochron (17b) for sample 01RB062 biotite.
*2σ **outside 95% confidence interval

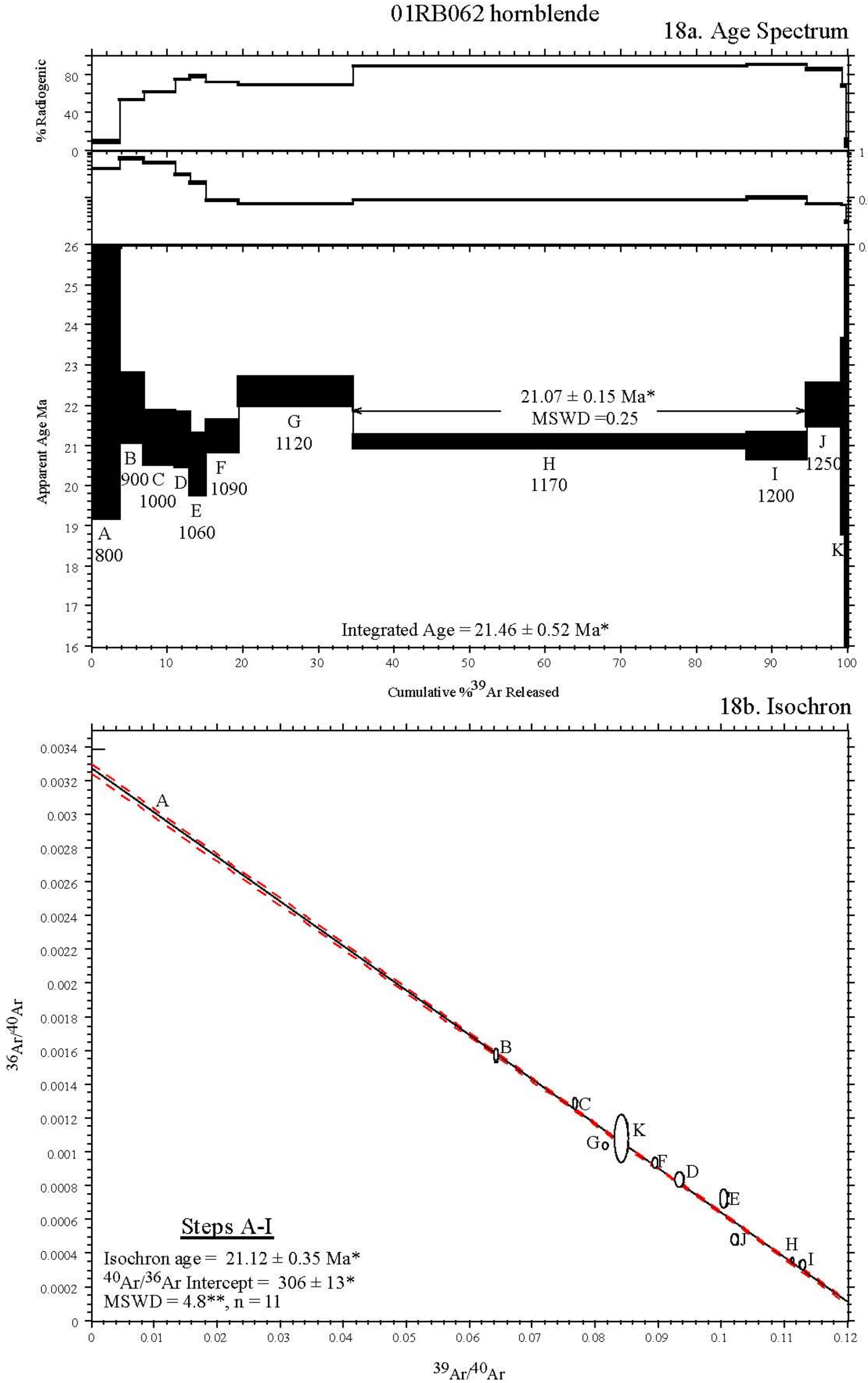

Figure 18. Age spectrum (18a) and isochron (18b) for sample 01RB062 hornblende.
*2σ **outside 95% confidence interval

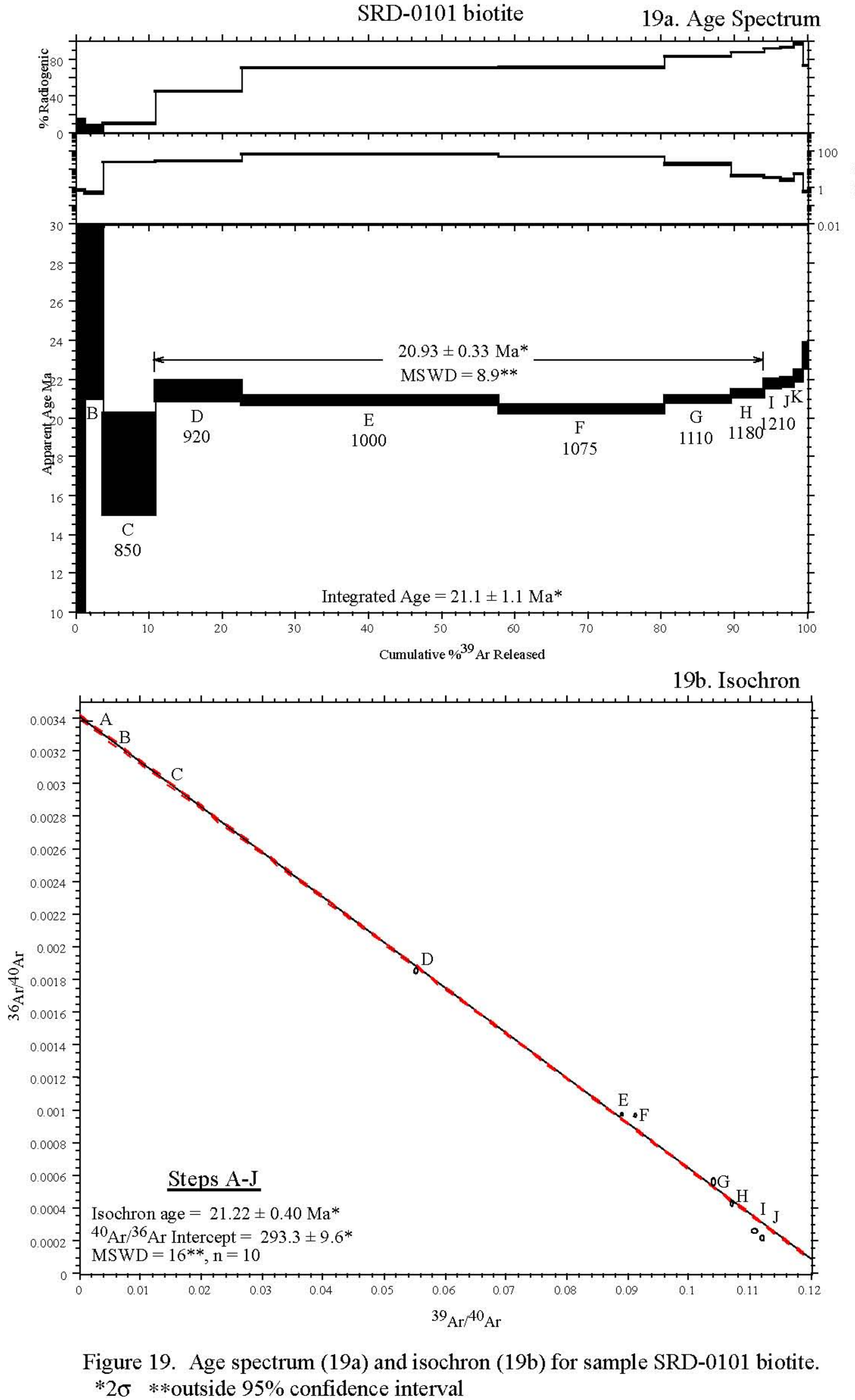

Figure 19. Age spectrum (19a) and isochron (19b) for sample SRD-0101 biotite. *2σ **outside 95% confidence interval

VY11802-7 Hornblende

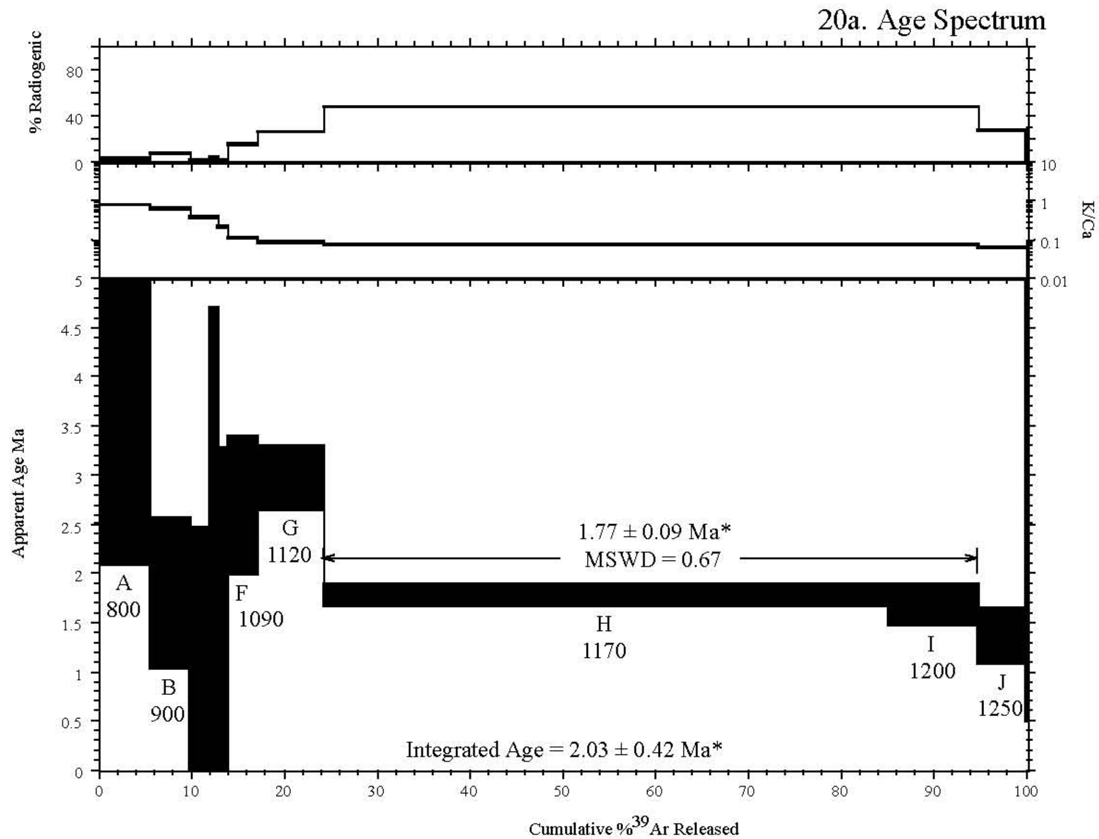

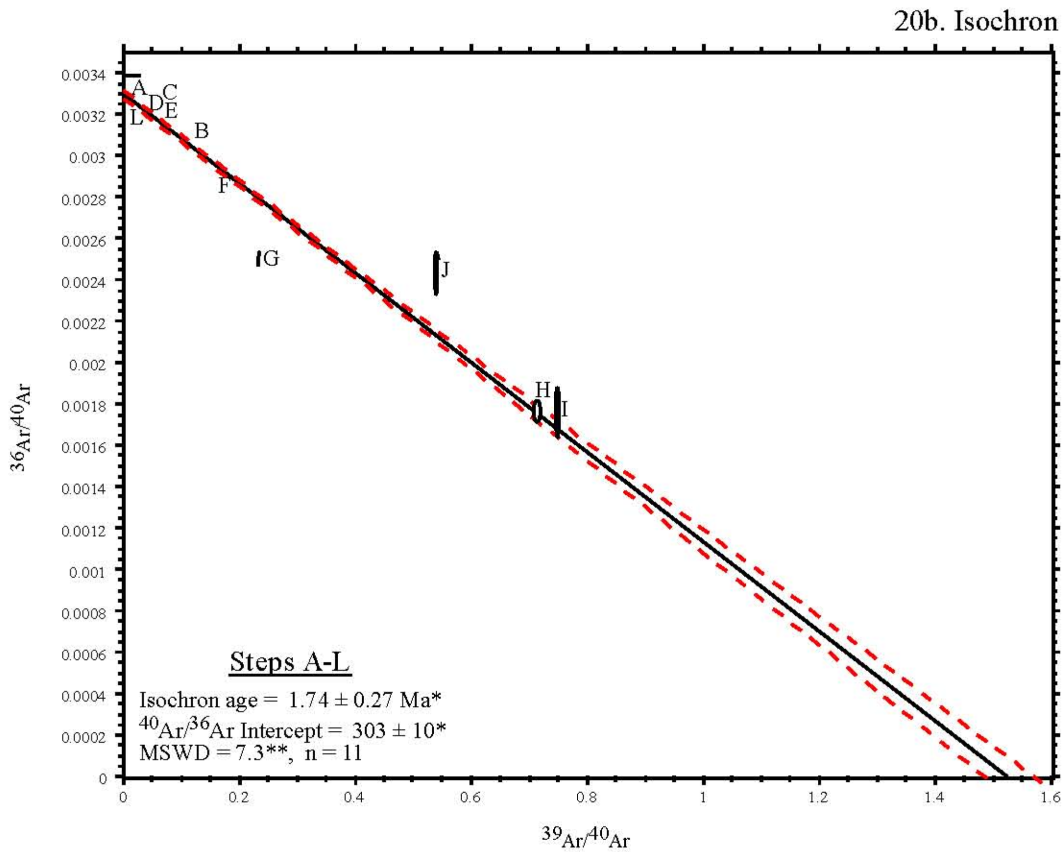

Figure 20. Age spectrum (20a) and isochron (20b) for sample VY11802-7 hornblende.
*2σ **outside 95% confidence interval

VY122001-3 Groundmass Concentrate

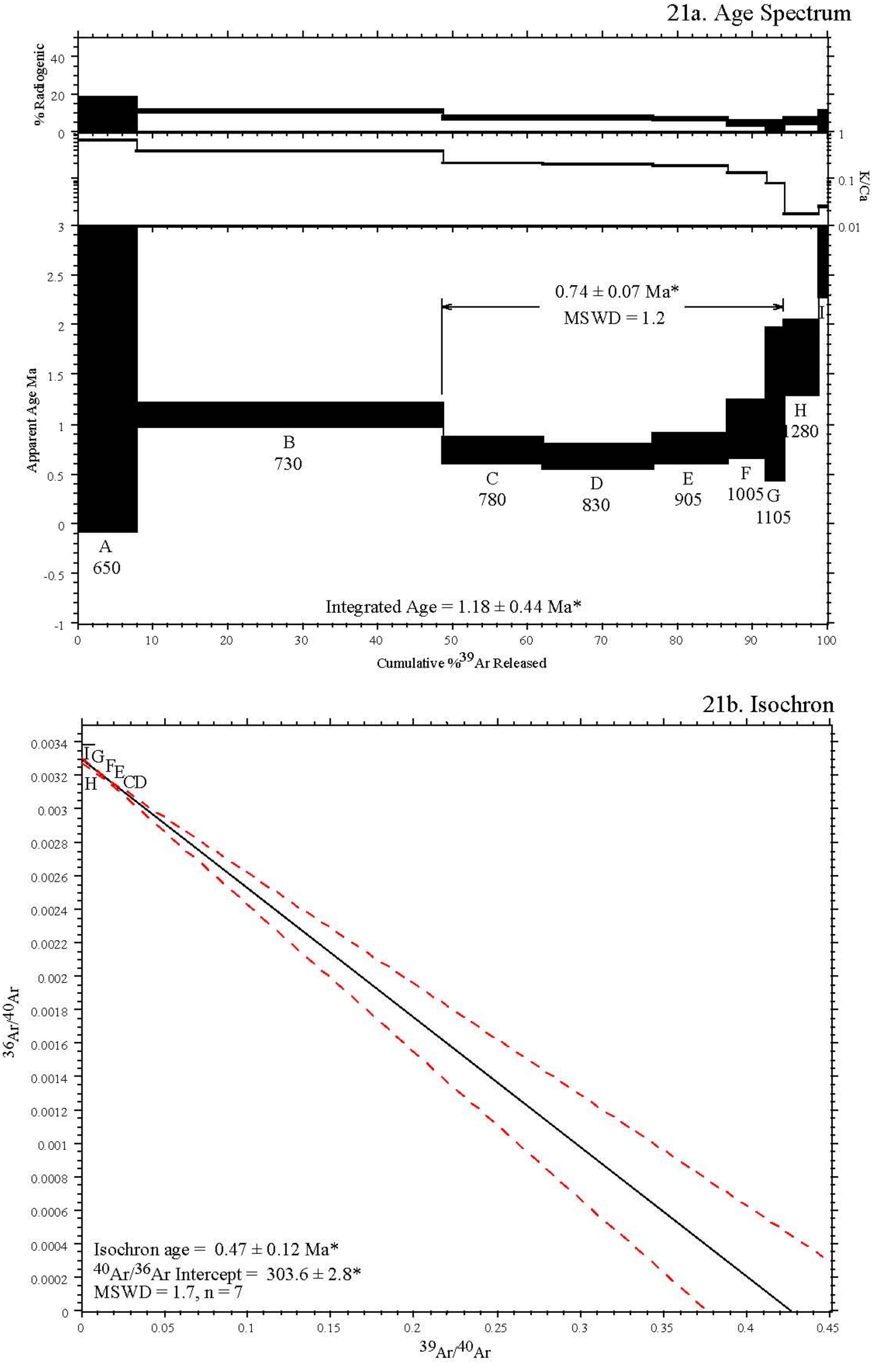

Figure 21. Age spectrum (21a) and isochron (21b) for sample VY122001-3 groundmass concentrate.
*2σ **outside 95% confidence interval

VY122001-9 Groundmass Concentrate

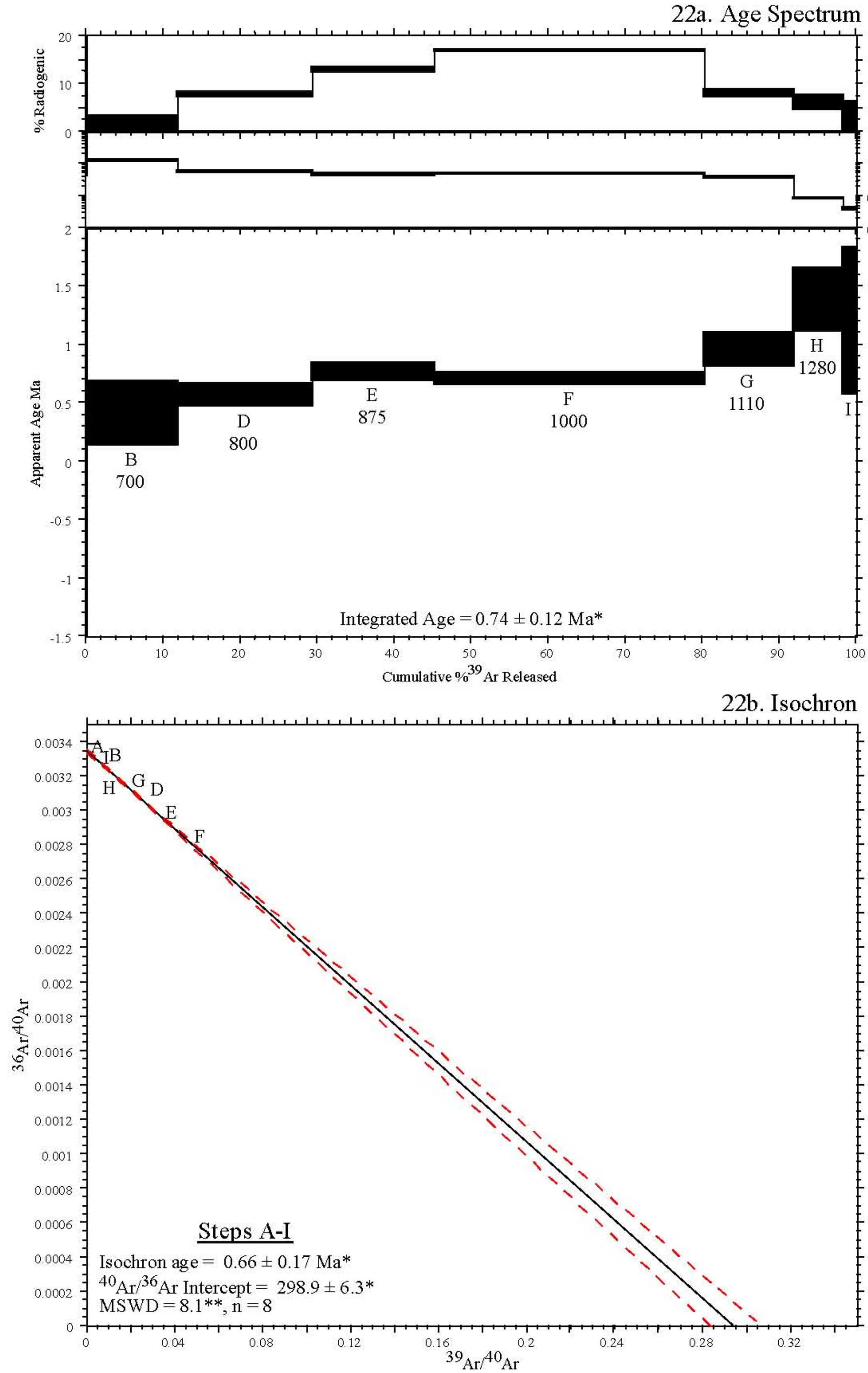

Figure 22. Age spectrum (22a) and isochron (22b) for sample VY122001-9 groundmass concentrate.
*2σ **outside 95% confidence interval

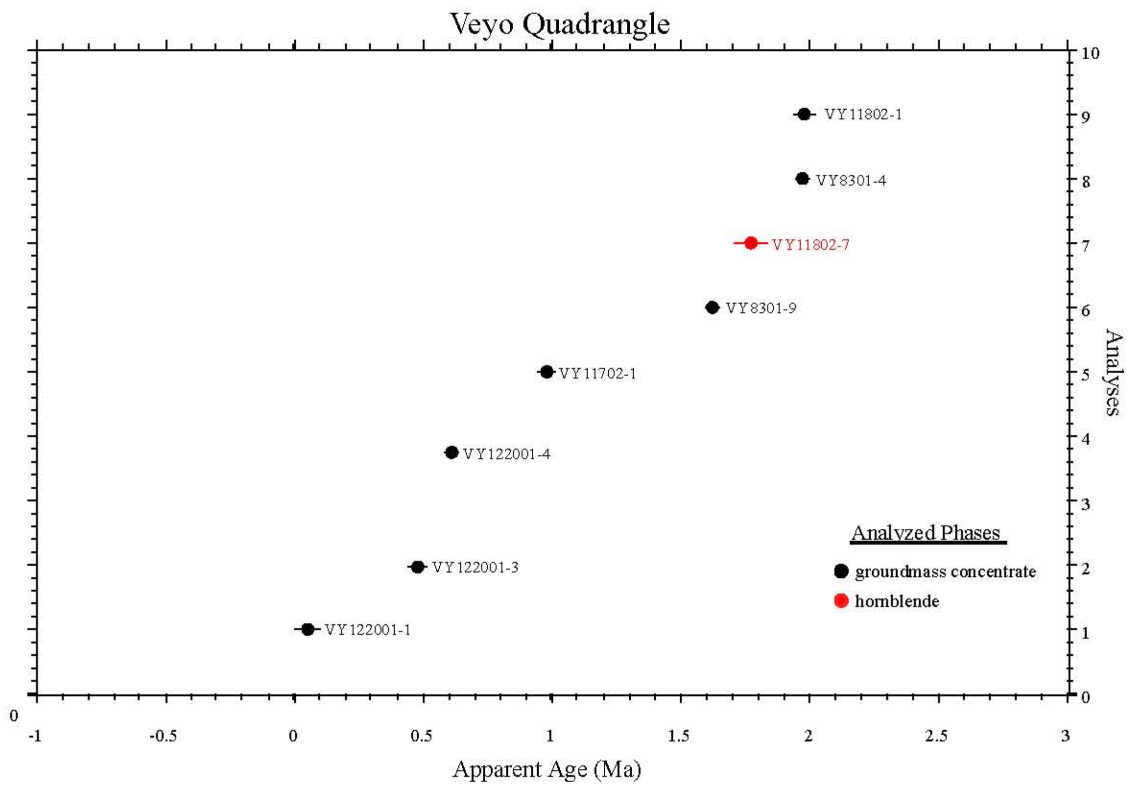

Figure 23. Summary of the Veyo quadrangle ages.

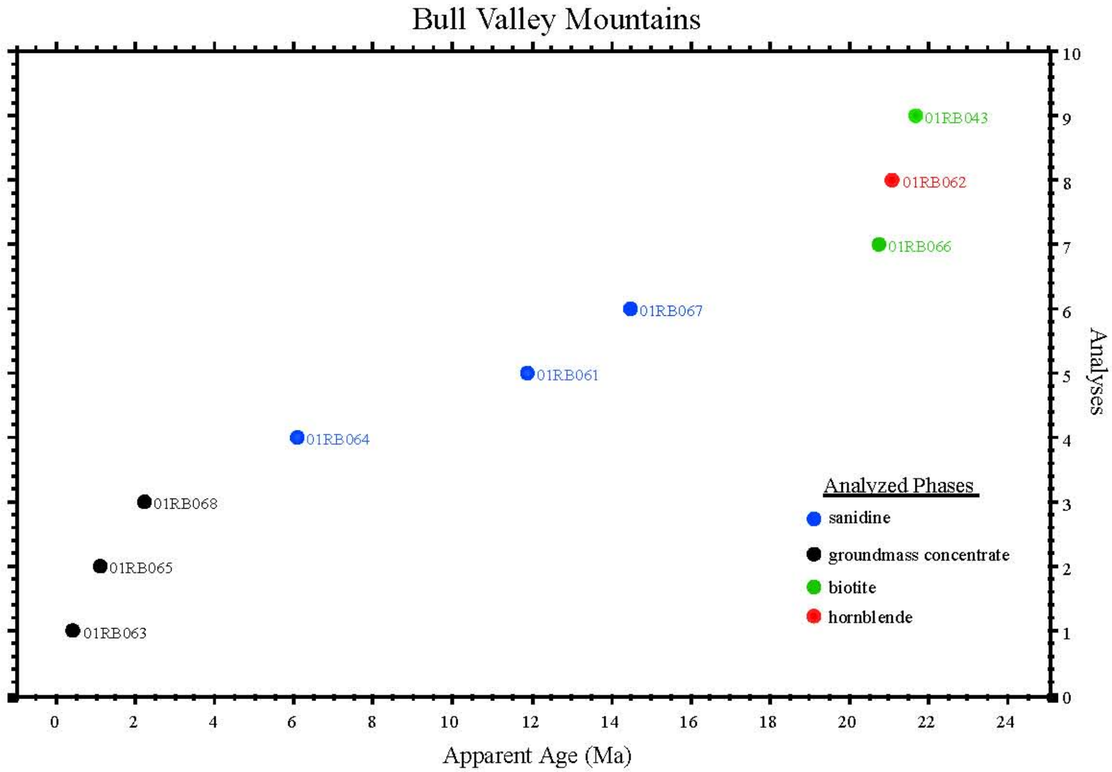

Figure 24. Summary of the Bull Valley Mountain ages.

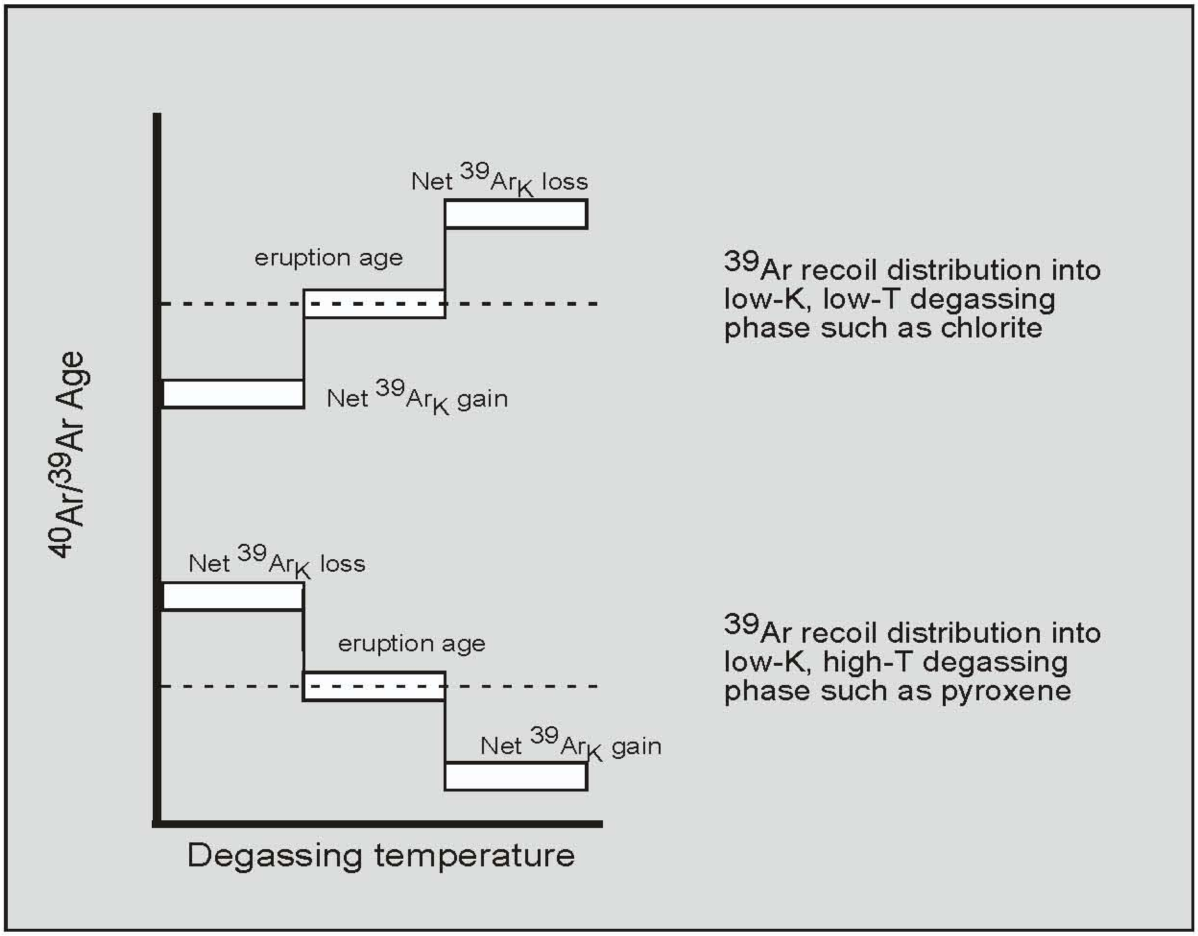

Figure 25. Cartoon showing potential effects of ^{39}Ar recoil on an otherwise flat age spectrum.

New Mexico Bureau of Mines and Mineral Resources

Procedures of the New Mexico Geochronology Research Laboratory

For the Period June 1998 – present

Matthew Heizler
William C. McIntosh
Richard Esser
Lisa Peters

$^{40}Ar/^{39}Ar$ and K-Ar dating

Often, large bulk samples (either minerals or whole rocks) are required for K-Ar dating and even small amounts of xenocrystic, authigenic, or other non-ideal behavior can lead to inaccuracy. The K-Ar technique is susceptible to sample inhomogeneity as separate aliquots are required for the potassium and argon determinations. The need to determine absolute quantities (i.e. moles of $^{40}Ar^*$ and ^{40}K) limits the precision of the K-Ar method to approximately 1% and also, the technique provides limited potential to evaluate underlying assumptions. In the $^{40}Ar/^{39}Ar$ variant of the K-Ar technique, a sample is irradiated with fast neutrons thereby converting ^{39}K to ^{39}Ar through a (n,p) reaction. Following irradiation, the sample is either fused or incrementally heated and the gas analyzed in the same manner as in the conventional K-Ar procedure, with one exception, no argon spike need be added.

Some of the advantages of the $^{40}Ar/^{39}Ar$ method over the conventional K-Ar technique are:

1. A single analysis is conducted on one aliquot of sample thereby reducing the sample size and eliminating sample inhomogeneity.
2. Analytical error incurred in determining absolute abundances is reduced by measuring only isotopic ratios. This also eliminates the need to know the exact weight of the sample.
3. The addition of an argon spike is not necessary.
4. The sample does not need to be completely fused, but rather can be incrementally heated. The $^{40}Ar/^{39}Ar$ ratio (age) can be measured for each fraction of argon released and this allows for the generation of an age spectrum.

The age of a sample as determined with the $^{40}Ar/^{39}Ar$ method requires comparison of the measured $^{40}Ar/^{39}Ar$ ratio with that of a standard of known age. Also, several isotopes of other elements (Ca, K, Cl, Ar) produce argon during the irradiation procedure and must be corrected for. Far more in-depth details of the determination of an apparent age via the $^{40}Ar/^{39}Ar$ method are given in Dalrymple et al. (1981) and McDougall and Harrison (1988).

Analytical techniques

Sample Preparation and irradiation details

Mineral separates are obtained in various fashions depending upon the mineral of interest, rock type and grain size. In almost all cases the sample is crushed in a jaw crusher and ground in a disc grinder and then sized. The size fraction used generally corresponds to the largest size possible which will permit obtaining a pure mineral separate. Following sizing, the sample is washed and dried. For plutonic and metamorphic rocks and lavas, crystals are separated using standard heavy liquid, Franz magnetic and hand-picking techniques. For volcanic sanidine and plagioclase, the sized sample is reacted with 15% HF acid to remove glass and/or matrix and then thoroughly washed prior to heavy liquid and magnetic separation. For groundmass concentrates, rock fragments are selected which do not contain any visible phenocrysts.

The NMGRL uses either the Ford reactor at the University of Michigan or the Nuclear Science Center reactor at Texas A&M University. At the Ford reactor, the L67 position is used (unless otherwise noted) and the D-3 position is always used at the Texas A&M reactor. All of the Michigan irradiations are carried out underwater without any shielding for thermal neutrons, whereas the Texas irradiations are in a dry location which is shielded with B and Cd. Depending upon the reactor used, the mineral separates are loaded into either holes drilled into Al discs or into 6 mm I.D. quartz tubes. Various Al discs are used. For Michigan, either six hole or twelve hole, 1 cm diameter discs are used and all holes are of equal size. Samples are placed in the 0, 120 and 240° locations and standards in the 60, 180 and 300° locations for the six hole disc. For the twelve hole disc, samples are located at 30, 60, 120, 150, 210, 240, 300, and 330° and standards at 0, 90, 180 and 270 degrees. If samples are loaded into the quartz tubes, they are wrapped in Cu foil with standards interleaved at ~0.5 cm intervals. For Texas, 2.4 cm diameter discs contain either sixteen or six sample holes with smaller holes used to hold the standards. For the six hole disc, sample locations are 30, 90, 150, 210, 270 and 330° and standards are at 0, 60, 120, 180, 240 and 300°. Samples are located at 18, 36, 54, 72, 108, 126, 144, 162, 198, 216, 234, 252, 288, 306, 324, 342 degrees and standards at 0, 90, 180 and 270 degrees in the sixteen hole disc. Following sample loading into the discs, the discs are stacked, screwed together and sealed in vacuo in either quartz (Michigan) or Pyrex (Texas) tubes.

Extraction Line and Mass Spectrometer details

The NMGRL argon extraction line has both a double vacuum Mo resistance furnace and a CO_2 laser to heat samples. The Mo furnace crucible is heated with a W heating element and the temperature is monitored with a W-Re thermocouple placed in a hole drilled into the bottom of the crucible. A one inch long Mo liner is placed in the bottom of the crucible to collect the melted samples. The furnace temperature is calibrated by either/or melting Cu foil or with an additional thermocouple inserted in the top of the furnace down to the liner. The CO_2 laser is a Synrad 10W laser equipped with a He-Ne pointing laser. The laser chamber is constructed from a 3 3/8" stainless steel conflat and the window material is ZnS. The extraction line is a two stage design. The first stage is equipped with a SAES GP-50 getter, whereas the second stage houses two SAES GP-50 getters and a tungsten filament. The first stage getter is operated at 450°C as is one of the second stage getters. The other second stage getter is operated at room temperature and the tungsten filament is operated at ~2000°C. Gases evolved from samples heated in the furnace are reacted with the first stage getter during heating. Following heating, the gas is expanded into the second stage for two minutes and then isolated from the first stage. During second stage cleaning, the first stage and furnace are pumped out. After gettering in the second stage, the gas is expanded into the mass spectrometer. Gases evolved from samples heated in the laser are expanded through a cold finger operated at -140°C and directly into the second stage. Following cleanup, the gas in the second stage and laser chamber is expanded into the mass spectrometer for analysis.

The NMGRL employs a MAP-215-50 mass spectrometer which is operated in static mode. The mass spectrometer is operated with a resolution ranging between 450 to 600 at mass 40 and isotopes are detected on a Johnston electron multiplier operated at ~2.1 kV with an overall gain of about 10,000 over the Faraday collector. Final isotopic intensities are determined by linear regression to time zero of the peak height versus time following gas introduction for each mass. Each mass intensity is corrected for mass spectrometer baseline and background and the extraction system blank.

Blanks for the furnace are generally determined at the beginning of a run while the furnace is cold and then between heating steps while the furnace is cooling. Typically, a blank is run every three to six heating steps. Periodic furnace hot blank analysis reveals that the cold blank is equivalent to the hot blank for temperatures less than about 1300°C. Laser system blanks are generally determined between every four analyses. Mass discrimination is measured using atmospheric argon which has been dried using a Ti-sublimation pump. Typically, 10 to 15 replicate air analyses are measured to determine a mean mass discrimination value. Air pipette analyses are generally conducted 2-3 times per month, but more often when samples sensitive to the mass discrimination value are analyzed. Correction factors for interfering nuclear reactions on K and Ca are determined using K-glass and CaF_2, respectively. Typically, 3-5 individual pieces of the salt or glass are fused with the CO_2 laser and the correction factors are calculated from the weighted mean of the individual determinations.

Data acquisition, presentation and age calculation

Samples are either step-heated or fused in a single increment (total fusion). Bulk samples are often step-heated and the data are generally displayed on an age spectrum or isochron diagram. Single crystals are often analyzed by the total fusion method and the results are typically displayed on probability distribution diagrams or isochron diagrams.

The Age Spectrum Diagram

Age spectra plot apparent age of each incrementally heated gas fraction versus the cumulative % $^{39}Ar_K$ released, with steps increasing in temperature from left to right. Each apparent age is calculated assuming that the trapped argon (argon not produced by *in situ* decay of ^{40}K) has the modern day atmospheric $^{40}Ar/^{36}Ar$ value of 295.5. Additional parameters for each heating step are often plotted versus the cumulative %$^{39}Ar_K$ released. These auxiliary parameters can aid age spectra interpretation and may include radiogenic yield (percent of ^{40}Ar which is not atmospheric), K/Ca (determined from measured Ca-derived ^{37}Ar and K-derived ^{39}Ar) and/or K/Cl (determined from measured Cl-derived ^{38}Ar and K-derived ^{39}Ar). Incremental heating analysis is often effective at revealing complex argon systematics related to excess argon, alteration, contamination, ^{39}Ar recoil, argon loss, etc. Often low-temperature heating steps have low radiogenic yields and apparent ages with relatively high errors due mainly to loosely held, non-radiogenic argon residing on grain surfaces or along grain boundaries. An entirely or partially flat spectrum, in which apparent ages are the same within analytical error, may indicate that the sample is homogeneous with respect to K and Ar and has had a simple thermal and geological history. A drawback to the age spectrum technique is encountered when hydrous minerals such as micas and amphiboles are analyzed. These minerals are not stable in the ultra-high vacuum extraction system and thus step-heating can homogenize important details of the true ^{40}Ar distribution. In other words, a flat age spectrum may result even if a hydrous sample has a complex argon distribution.

The Isochron Diagram

Argon data can be plotted on isotope correlation diagrams to help assess the isotopic composition of Ar trapped at the time of argon closure, thereby testing the assumption that trapped argon isotopes have the composition of modern atmosphere which is implicit in age spectra. To construct an "inverse isochron" the $^{36}Ar/^{40}Ar$ ratio is plotted versus the $^{39}Ar/^{40}Ar$ ratio. A best fit line can be calculated for the data array which yields the value for the trapped argon (Y-axis intercept) and the $^{40}Ar^*/^{39}Ar_K$ value (age) from the X-axis intercept. Isochron analysis is most useful for step-heated or total fusion data which have a significant spread in radiogenic yield. For young or low K samples, the calculated apparent age can be very sensitive to the composition of the trapped argon and therefore isochron analysis should be preformed routinely on these samples (cf. Heizler and Harrison, 1988). For very old (>Mesozoic) samples or relatively old sanidines (>mid-Cenozoic) the data are often highly radiogenic and cluster near the X-axis thereby making isochron analysis of little value.

The Probability Distribution Diagram

The probability distribution diagram, which is sometimes referred to as an ideogram, is a plot of apparent age versus the summation of the normal distribution of each individual analysis (Deino and Potts, 1992). This diagram is most effective at displaying single crystal laser fusion data to assess the distribution of the population. The K/Ca, radiogenic yield, and the moles of ^{39}Ar for each analysis are also often displayed for each sample as this allows for visual ease in identifying apparent age correlations between, for instance, plagioclase contamination, signal size and/or radiogenic concentrations. The error (1σ) for each age analysis is generally shown by the horizontal lines in the moles of ^{39}Ar section. Solid symbols represent the analyses used for the weighted mean age calculation and the generation of the solid line on the ideogram, whereas open symbols represent data omitted from the age calculation. If shown, a dashed line represents the probability distribution of all of the displayed data. The diagram is most effective for displaying the form of the age distribution (i.e. gaussian, skewed, etc.) and for identifying xenocrystic or other grains which fall outside of the main population.

Error Calculations

For step-heated samples, a plateau for the age spectrum is defined by the steps indicated. The plateau age is calculated by weighting each step on the plateau by the inverse of the variance and the error is calculated by either the method of Samson and Alexander (1987) or Taylor (1982). A mean sum weighted deviates (MSWD) value is determined by dividing the Chi-squared value by n-1 degrees of freedom for the plateau ages. If the MSWD value is outside the 95% confidence window (cf. Mahon, 1996; Table 1), the plateau or preferred age error is multiplied by the square root of the MSWD.

For single crystal fusion data, a weighted mean is calculated using the inverse of the variance to weight each age determination (Taylor, 1982). Errors are calculated as described for the plateau ages above.

Isochron ages, $^{40}Ar/^{36}Ar_i$ values and MSWD values are calculated from the regression results obtained by the York (1969) method.

References cited

Dalrymple, G.B., Alexander, E.C., Jr., Lanphere, M.A., and Kraker, G.P., 1981. Irradiation of samples for $^{40}Ar/^{39}Ar$ dating using the Geological Survey TRIGA reactor. U.S.G.S., Prof. Paper, 1176.

Deino, A., and Potts, R., 1990. Single-Crystal $^{40}Ar/^{39}Ar$ dating of the Olorgesailie Formation, Southern Kenya Rift, J. Geophys. Res., 95, 8453-8470.

Deino, A., and Potts, R., 1992. Age-probability spectra from examination of single-crystal $^{40}Ar/^{39}Ar$ dating results: Examples from Olorgesailie, Southern Kenya Rift, Quat. International, 13/14, 47-53.

Fleck, R.J., Sutter, J.F., and Elliot, D.H., 1977. Interpretation of discordant $^{40}Ar/^{39}Ar$ age-spectra of Mesozoic tholieiites from Antarctica, Geochim. Cosmochim. Acta, 41, 15-32.

Heizler, M. T., and Harrison, T. M., 1988. Multiple trapped argon components revealed by $^{40}Ar/^{39}Ar$ analysis, Geochim. Cosmochim. Acta, 52, 295-1303.

Mahon, K.I., 1996. The New "York" regression: Application of an improved statistical method to geochemistry, International Geology Review, 38, 293-303.

McDougall, I., and Harrison, T.M., 1988. Geochronology and thermochronology by the ^{40}Ar-^{39}Ar method. Oxford University Press.

Samson, S.D., and, Alexander, E.C., Jr., 1987. Calibration of the interlaboratory $^{40}Ar/^{39}Ar$ dating standard, Mmhb-1, Chem. Geol., 66, 27-34.

Steiger, R.H., and Jäger, E., 1977. Subcommission on geochronology: Convention on the use of decay constants in geo- and cosmochronology. Earth and Planet. Sci. Lett., 36, 359-362.

Taylor, J.R., 1982. An Introduction to Error Analysis: The Study of Uncertainties in Physical Measurements,. Univ. Sci. Books, Mill Valley, Calif., 270 p.

York, D., 1969. Least squares fitting of a straight line with correlated errors, Earth and Planet. Sci. Lett.., 5, 320-324.